INHIBITION OF STAT3 DECREASES OSM INDUCED EDA-FN EXPRESSION IN HUMAN LUNG FIBROBLASTS

by

JOYCE TSE

B.Sc., The University of British Columbia, 2008

A THESIS SUBMITTED IN PARTIAL FULFILLMENT OF
THE REQUIREMENTS FOR THE DEGREE OF

MASTER OF SCIENCE

in

THE FACULTY OF GRADUATE STUDIES

(Pharmacology and Therapeutics)

THE UNIVERSITY OF BRITISH COLUMBIA

(Vancouver)

April 2011

© Joyce Tse, 2011

ABSTRACT

Fibrosis is excessive deposition of connective tissue components that results in the destruction of normal tissue architecture and compromises organ function. When fibrosis occurs in the major organs such as the lung, for example in idiopathic pulmonary fibrosis (IPF), it inevitably leads to organ failure and premature death of the afflicted individual. The development of fibrosis follows a similar pathway to normal wound healing, although there is chronic progression of the disease without resolution, suggesting the fine control of cellular functions that occur during wound healing is disturbed. Determining where this control is lost is paramount to preventing and treating this condition. Fibroblasts are the main cell type responsible for extracellular matrix (ECM) production. The transcription factor signal-transducer-and-activator-of-transcription-3 (STAT-3) regulates genes involved in cell differentiation and wound healing. It has been shown that fibroblasts isolated from normal and IPF lungs differ in STAT3 dependent interleukin-6 (IL-6)/glycoprotein 130 (gp130) cell signaling and proliferation. Therefore, we aimed to evaluate whether STAT3 inhibition could decrease expression of ECM proteins, including collagen and extra-domain A fibronectin (EDA-FN) in human lung fibroblasts. We also sought to examine the effect of knocking down STAT3 function on fibroblast proliferation. Cells were exposed to Oncostatin-M (OSM) or IL-6, and collagen-1 and EDA-FN protein expression was analyzed by western blotting, while cell proliferation was assessed by bromo-deoxyuridine (BrdU) incorporation. STAT3 function was inhibited in two ways: Firstly, inhibition with a small molecule inhibitor, STA-21, blocks STAT3 dimerization and nuclear translocation and secondly, inhibition of STAT3 gene transcription by

short interfering RNA (siRNA). Both methods inhibited OSM induced EDA-FN expression and proliferation in human fetal lung (HFL) fibroblasts. However, STAT3 had negligible effects in adult lung fibroblasts. We attempted to resolve the disparate effects by inhibiting another downstream signaling pathway, the extracellular receptor kinase (ERK)-1/2, which is also activated by gp130. In conclusion, OSM induced EDA-FN expression and cell proliferation in HFL fibroblasts are dependent upon STAT3 activation. In contrast, STAT3 has minimal involvement in adult cells. The mechanisms underlying these disparate effects remain to be elucidated. Interestingly, inhibiting either STAT3 or ERK1/2 inhibited OSM induced proliferation in HFL fibroblasts.

TABLE OF CONTENTS

LIST OF FIGURES

LIST OF ABBREVIATIONS

AcEEED	Acetylated glutamic acid (x3)-aspartic acid sequence
AP-1	activated protein-1
BALF	Bronchoalveolar fluid
CLC	Cardiotrophin-like cytokine
CNTF	Ciliary neurotrophic factor
CT-1	Cardiotrophin-1
DAPI	4’,6-diamidino-2-phenylindole
DMEM	Dulbecco’s modified eagle medium
DMSO	Dimethyl sulfoxide
ECM	Extracellular matrix
EDA-FN	Extra-domain-A fibronectin
ERK1/2	Extracellular receptor kinase
EMT	Epithelial-mesenchymal transition
FBS	Fetal bovine serum
FGF	Fibroblast growth factor
gp130	Glycoprotein-130
HFL	Human fetal lung fibroblast
I/Iso	Isoleucine amino acid residue
IIP	Idiopathic interstitial pneumonia
ILD	Interstitial lung disease
IL-1	Interleukin-1
IL-6	Interleukin-6

IPF	Idiopathic pulmonary fibrosis
LIF	Leukemia inhibitory factor
LIFR	Leukemia inhibitory factor receptor
MAPK	Mitogen-activated protein kinase
MMP	Metalloproteinase
MORE	Oncostatin-M responsive element
OSM	Oncostatin-M
OSMR	Oncostatin-M receptor
PDGF	Platelet derived growth factor
PIAS	Protein inhibitor of activated STAT
pSTAT3	Phosphorylated STAT3
R/Arg	Arginine amino acid residue
RGD	Argine-glycine-aspartic acid
ROS	Reactive oxygen species
SH2	Src homology-2
siRNA	Short interfering RNA
SHP2	SH2-domain-containing tyrosine phosphatase
SNP	Short nucleotide polymorphism
SOCS	Suppressor of cytokine signalling
STAT3	Signal transducer and activator of transcription-3
TGF	Transforming growth factor
TGFβ1	Transforming growth factor-beta-1
TNF	Tumor necrosis factor

UIP	Usual interstitial pneumonia
Y/Tyr	Tyrosine amino acid residue
α-SMA	Alpha-smooth muscle actin

ACKNOWLEDGEMENTS

I would like to thank my principal investigator and supervisor, Dr. Darryl Knight, for providing me with the opportunity to participate in a research project in his lab and also my co-supervisor, Dr. Dmitri Peckovsky, for teaching and facilitating laboratory techniques. I would also like to thank the rest of the Knight Lab for continuous and extraordinary support both academically and outside the laboratory. I am grateful for their friendly advice.

I am also thankful to The Providence Heart and Lung Institute for providing excellent facilities and equipment to carry-out my experiments properly. The Knight and Bernatchez Labs have contributed significantly to my professional and personal growth.

The Anesthesiology, Pharmacology and Therapeutics department at The University of British Columbia must also be thanked for their high level of expectation, which have contributed to my academic success.

I would also like to thank my family for being considerate while I was pursuing this course of study.

Chapter 1. Introduction

1.1. Anatomy of the lung

The lung interstitium includes the alveolar epithelium, interstitial space, basement membrane and pulmonary capillary endothelium (Figure 1). The interstitial space is comprised of cells called fibroblasts. Fibroblasts are long spindle shaped cells with cytoplasm containing protrusions and have abundant rough endoplasmic reticulum, which signifies an augmented capacity to synthesize and secrete precursors of ECM proteins. In particular, fibroblasts continuously secrete collagen and the glycoprotein fibronectin, and these ECM proteins regulate tissue tension and determine the integrity of lung connective tissue, which impacts on gas exchange and lung function (Hinz *et al.* 2007).

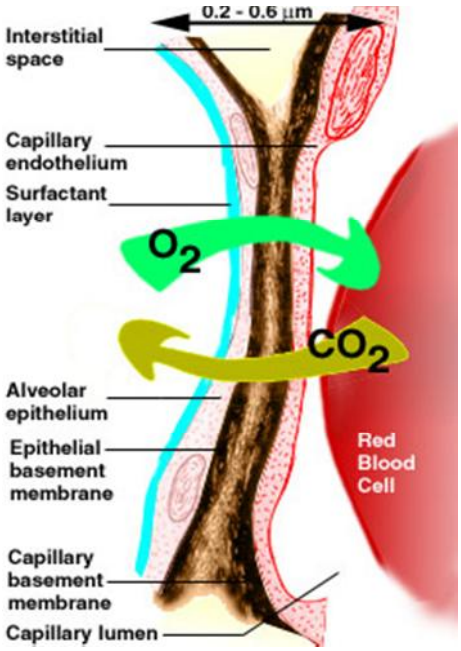

Figure 1. Gas diffusion across the lung alveolar epithelium and capillary endothelium. The junction between the alveolar epithelium and capillary endothelium is thin-walled to allow efficient gas transfer (Adopted from McGill University Physiology Department lecture notes).

1.2. Pulmonary fibrosis: Disease classification, etiology and prevalence

There are two types of fibrotic diseases: systemic or organ-specific (Rosenbloom *et al*. 2010). Systemic fibrotic diseases include multiple sclerosis, multifocal fibrosclerosis and sclerodermatous bone marrow. Organ-specific diseases include pulmonary, liver and kidney fibrosis. Despite differences in their etiology, they share the common feature of enhanced deposition of ECM in the affected tissues.

Lung diseases are either classified as an interstitial lung disease (ILD), also known as diffuse parenchymal lung disease, or an obstructive airway disease (du Bois 2010). The underlying

causes of ILD may include prolonged environmental exposure to silica (silicosis), asbestos (asbestosis), adverse drug effects (e.g. bleomycin), systemic illnesses (e.g. AIDS) or radiation exposure (du Bois 2010). Furthermore, ILD are subdivided into four subtypes of which one is idiopathic interstitial pneumonia (IIP). The most common form of IIP is idiopathic pulmonary fibrosis (IPF), in which the histological pattern is referred to as usual interstitial pneumonia (UIP). IPF/UIP is the most unresponsive to current therapies (Khalil & O'Connor 2004). Current epidemiological studies suggest that IPF is more common in male subjects, with onset in middle age (Khalil & O'Connor 2004). There are no distinct geographic, racial or ethnic group distributions of the disease. Although the precise etiology is unknown, a number of risk factors may contribute to disease development, such as smoking, silica and asbestos, and in familial cases, these include genetic abnormalities associated with telomerase dysfunction (Armannios *et al.* 2007) and surfactant protein C (Thomas *et al*. 2002). End stage disease is characterized by abnormal parenchymal tissue remodelling, myofibroblast persistence, excessive deposition of collagen and other ECM components, aberrant re-epithelialization and angiogenesis, with a consequent progressive destruction of normal lung tissue (honeycombing), rapid loss of lung function and premature death (King *et al.* 2001). The specific molecular and cellular mechanisms that contribute to disease progression are unknown, although considerable effort is being made to delineate these pathological processes. The most recently accepted hypothesis is that aberrant wound healing responses through dysregulated epithelial – mesenchymal cross-talk are major contributors (Selman *et al.* 2001). There is no cure for this disease and despite aggressive treatment with immunosuppressants and anti-inflammatory agents such as corticosteroids, the three-year survival rate is still < 50% (Khalil & O'Connor 2004).

1.3. Fibroblasts

Fibroblasts are the primary cells appear in all organs of the body in animals (Jeon 2009) and are predominantly found beneath the basement membrane underlining the epithelium. Fibroblasts function to establish, maintain and modify the framework of connective tissue. In addition to secreting structural ECM proteins, such as collagen and fibronectin, they produce proteinases to organize and remodel the ECM and other non-structural ECM proteins to communicate with adjacent cells via autocrine and paracrine processes. During wound healing, fibroblasts migrate, increase their rate of proliferation and differentiate into protomyofibroblasts and ultimately into myofibroblasts. At this stage, myofibroblasts are generally thought to increase synthesis of ECM proteins and upregulate α-smooth muscle actin (α-SMA) fibers to contract the newly deposited ECM during the resolution phase of wound healing (Figure 2). Protomyofibroblasts and fully activated myofibroblasts are distinguished by their expression of α-SMA stress fibers (Hinz *et al.* 2007), in which protomyofibroblasts contain mostly β- and γ-cytosolic actin and little α-SMA and myofibroblasts have well-organized α-SMA that promotes cell contractility (Hinz *et al.* 2007). α-SMA stress fibers contain an N-terminal amino acid sequence AcEEED that can generate more than two-fold contractile force compared to β- and γ-cytosolic actin. As such, α-SMA is commonly used as a biological marker for detection of myofibroblasts. The α-SMA fibers are connected with the ECM at focal adhesion sites and between cells via adhesion junctions. ECM rigidity determines the size of the adhesion anchor sites and the amount of tension generated by the stress fibers. Usual focal adhesion sites range from 2 to 6 μm long. Increased ECM substrate rigidity, for example, during wound healing, induces the formation of supermature focal adhesions and allows α-SMA to incorporate into pre-existing β- and γ-cytosolic actin to generate a myofibroblast that potentially has a four-fold increase in contractile

force (Hinz *et al.* 2007). In normal wound healing, after the wound has repaired, myofibroblasts are thought to undergo apoptosis and the ECM returns to normal homeostatic levels with a repaired and intact epithelium.

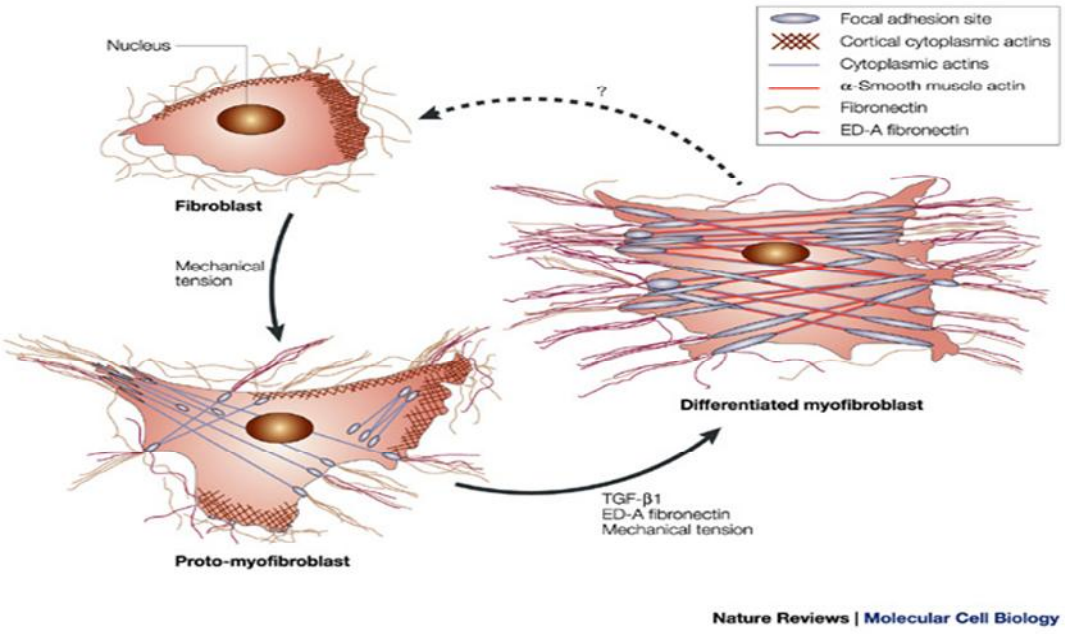

Figure 2. Differentiation of fibroblasts during wound healing. Fibroblasts differentiate into myofibroblasts during the wound healing process to enhance the expression of extracellular matrix proteins and to contract the site of injury to prevent excessive haemorrhage (Tomosek *et al.* 2002).

1.4. Pathogenesis of pulmonary fibrosis

Damage to alveolar epithelial cells is thought to be the initial event that triggers the normal wound repair process. Resident macrophages are the first responders, which secrete transforming growth factor (TGF-β1), tumor necrosis factor-α (TNFα), pro-inflammatory cytokines (IL-1 and IL-6) and chemokines (Elias *et al.* 1990). IL-1 and TNFα upregulate adhesion molecule expression on endothelial cells to attract and bind neutrophils and increase vascular permeability to allow neutrophil penetration from the vascular lumen into the tissues. TNFα also promotes chemotaxis and activation of neutrophils so that neutrophils are recruited to

the injured site within minutes, which release reactive oxygen species (ROS). Monocytes are also recruited and mature into active macrophages to enhance to wound repair process. Damage to the basement membrane and capillary endothelium causes leakage of coagulant factors from the blood circulation into the alveolar space. Activated platelets release platelet derived growth factor (PDGF), TGFβ1 and basic fibroblast growth factor (bFGF).

TGFβ1 induces the differentiation of fibroblasts into myofibroblasts. As aforementioned, myofibroblasts undergo apoptosis in normal wound healing and their associated ECM proteins degrade to physiological levels. However, in pathological conditions, myofibroblasts fail to undergo apoptosis and thus, aggregate and localize into regions known as "myofibroblastic foci," as recognized by their high density of positive α-SMA that is seen in IPF histological lung sections. Identification of a myofibroblastic focus is an essential and distinctive morphological feature of IPF (Hinz *et al.* 2007). The extent of these foci is also a reliable indicator of survival in IPF. These differentiated fibroblasts are likely to play a key role in the progression of IPF and as such strategies that modulate the expansion and function of these cells may have a significant impact on the treatment of the disease**.** However, the origin of these cells in IPF remains a mystery. In addition to expansion and transition of resident fibroblasts, myofibroblasts may originate from at least 3 other sources: circulating fibrocytes, epithelial-mesenchymal transition (EMT) and de-differentiation of stromal cells.

1.5. Extracellular matrix proteins and fibronectin

Collagen is the most abundant protein in the ECM. There are more than sixteen types of collagen, but fibroblasts secrete collagen types I, III, VI, VIII, IX and X. They appear in the

structural forms of fibrillar, non-fibrillar, short-chain and fibril-associated collagen with interrupted triple helices (FACIT). Fibrillar collagen produced by fibroblasts is most abundant in the mammalian body. Collagen is initially transcribed into a pre-procollagen, followed by post-translational modification that includes hydroxylation and glycosylation of proline and lysine residues. This results in a fibrillar protein known as an alpha chain that consists of repeating amino acid triplets of glycine-X-Y, where every third X is a proline and every third Y is hydroxyproline. Assembly of three alpha chains forms a pro-collagen triple-helix that is secreted into the extracellular matrix and further cleaved into a collagen molecule. Self-assembly of collagen molecules forms a fibril, and aggregation of collagen fibrils form a collagen fiber that provides structural support to cells and tissues. Collagen undergoes a continuous cycle of synthesis and degradation throughout life. Approximately 10% of total lung collagen content is being synthesized and degraded daily (McAnulty & Laurent 1987). Collagen is degraded via basal degradation or enhanced degradation (Berg *et al.* 1980). Basal degradation occurs when there are optimal conditions for proline hydroxylation. Enhanced degradation occurs when conditions prevent proline hydroxylation. Accumulation of type I collagen leads to organ dysfunction in fibrosis.

Fibronectin is another important structural component of the ECM. Fibronectin is secreted by various cell types, but mostly fibroblasts. It is secreted as an unfolded, inactive glycoprotein monomer, which is activated upon dimerization. This is also known as cellular fibronectin, which contrasts the plasma fibronectin that is produced by liver hepatocytes. Despite its name, cellular fibronectin is found both intracellularly and extracellularly. Fibronectin is involved in cytoskeletal organization, cell adhesion, spreading and migration by functioning as linkers

between cells and various extracellular proteins, such as heparin, fibrin, actin and collagen (Odenthal *et al*. 1993). Cellular and plasma fibronectin are expressed by the same gene, but are different splice variants. Fibronectin interacts and communicates with fibroblasts via cell surface receptors called integrins. Binding to specific α5β1 integrins facilitates fibronectin monomers to form active dimers, which then assemble into fibrillar networks and act as adaptor proteins that connect fibroblasts to collagen fibers (Singh *et al*. 2010). Fibronectin is also referred to as a mechanical protein as it allows fibroblasts to detect the mechanical tension in the ECM (via integrins) and facilitates cell migration when a change in mechanical tension is detected.

Dimers of fibronectin are linked by a pair of C-terminal disulfide bonds with a molecular weight of approximately 440 kDa (Mao & Schwarzbauer 2005). The monomer consists of three domains: type I, type II and type III (Figure 3). Different domains accounts for the wide binding capability of fibronectin (e.g. heparin, collagen, fibrin). The type III domain contains 13 modules. The 10^{th} module contains an RGD amino acid sequence that mediates its binding to the integrin receptor. The type III domain may also contain two connecting segment (III CS) subdomains, referred to as "extra" type A or B (EDA or EDB). Fibronectin containing the extra type A subdomain is called cellular fibronectin or EDA-fibronectin (EDA-FN). Expression of EDA-FN induces the formation of α-SMA-positive and differentiation of fibroblasts into myofibroblasts (Kohan *et al.* 2010). Thus, aberrant fibronectin function, as a result of increased expression, reduced degradation and/or improper organization, has been associated with the pathogenesis of cancer and fibrosis (Williams *et al*. 2008). In particular, there is increased cellular fibronectin expression in liver fibrosis (Odenthal *et al.* 1993).

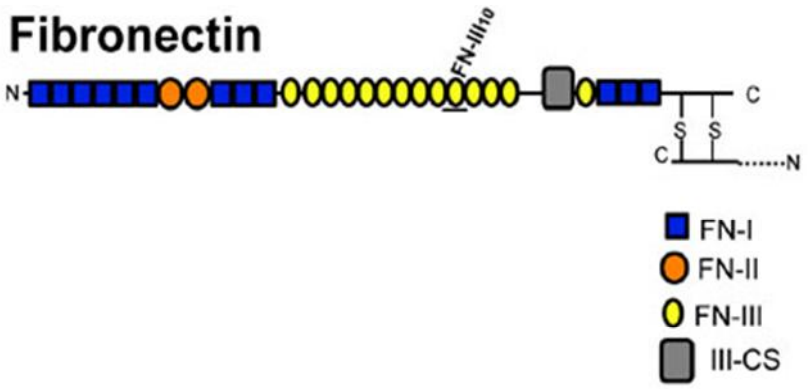

Figure 3. Schematic diagram of a fibronectin monomer. A fibronectin monomer contains three domains: first (blue), second (orange) and third (yellow). Within domain three includes an integrin receptor binding site in the 10th module (FN-III10) and a subdomain (III-CS), rendering EDA or EDB fibronectin. Fibronectin monomer dimerizes via dicysteine bonds.

1.6. Role of Interleukin-6 family cytokine signalling in inflammation and fibrosis

One potential signalling pathway that leads to pro-fibrotic fibroblast function is the interleukin-6 (IL-6) pathway (Heinrich *et al*. 2003). IL-6 is an acute phase response cytokine produced and secreted by macrophages, T helper cells, B cells, astrocytes and endothelial cells in response to tissue injury. It acts as both a pro- and anti-inflammatory cytokine in autocrine and paracrine communication. As a pro-inflammatory cytokine, IL-6 induces differentiation of T and B cells to initiate antibody production. As an anti-inflammatory cytokine, it inhibits the activity of pro-inflammatory cytokines TNFα and IL-1 and activates the anti-inflammatory protein IL-1 receptor antagonist and cytokine IL-10. IL-6 belongs to a family of closely related pleiotropic cytokines that activate a common signal-transducing transmembrane receptor subunit called

glycoprotein-130 (gp130). The other members of this family include IL-6, IL-11, leukemia inhibitory factor (LIF), oncostatin-M (OSM), ciliary neurotrophic factor (CNTF), cardiotrophin-1 (CT-1), cardiotrophin-like cytokine (CLC) and IL-31. IL-6 and IL-11 activate unique cell surface receptors, namely, IL-6 α chain and IL-11 α chain, respectively, and signal via gp130 homodimerization (Figure 4). In contrast, LIF, CT-1, CNTF, CLC and OSM signal via heterodimers of gp130 and LIF receptor (LIFR). OSM can also signal through heterodimers of gp130 and the OSM receptor (OSMR).

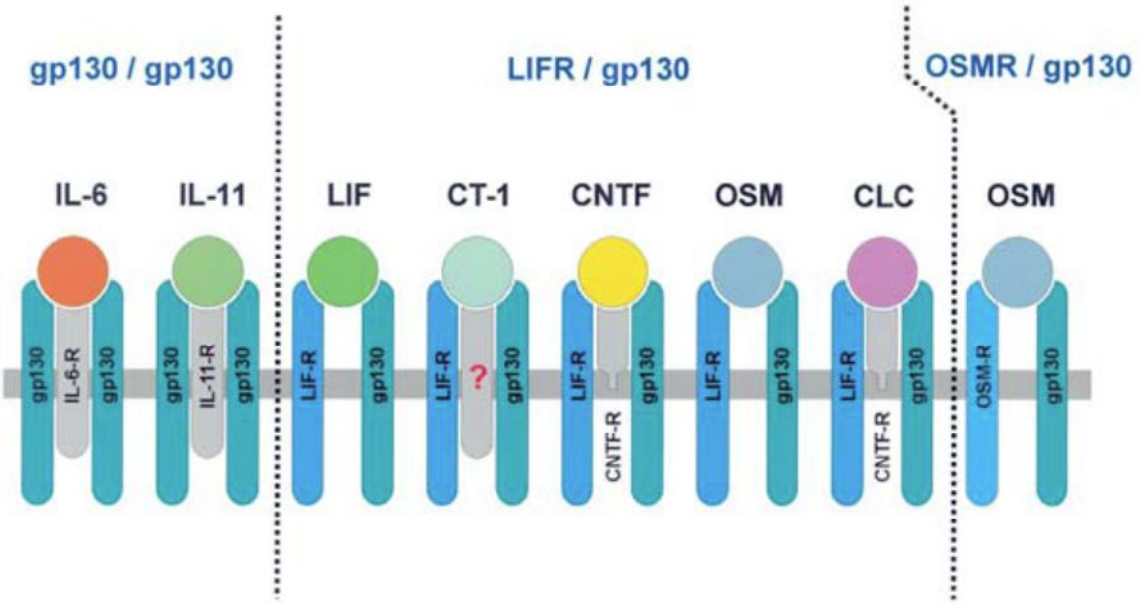

Figure 4. Receptor complexes of IL-6 type family cytokines. IL-6 type family cytokines signal through different receptor complexes that include gp130, LIF-R and OSM-R. All IL-6 type receptors contain a common gp130 subunit (Heinrich *et al.* 2003). IL-27 and IL-31 (not shown) contains to OSMR/gp130. Circle = ligand

Sequence identity between gp130, OSMR and LIFR is rather low, approximately 4.6% across the group (Taga & Kishimoto 1997). But as with most other type I cytokine receptors, they have two conserved short amino acid motifs in their intracellular domain named Box 1 and Box 2 (rich in proline residues). It is through these boxes that allow recruitment and activation of

receptor associated kinases: JAK1, JAK 2 or TYK2. A less conserved amino acid motif is called Box 3 (Kuropatwinski *et al.* 1997). Box 3 is necessary for the action of OSMR, but it is not required for signaling by the LIFR and gp130. Furthermore, the number and position of tyrosine residues available for phosphorylation in the cytoplasmic portion of the three receptor subunits vary. OSMR and LIFR share three homologous tyrosine residues, but none of these are found in gp130. LIFR contains LIFRβ and gp130 subunits. There are two types of OSMR: type I and type II. Type I OSMR is similar to LIFR (gp130 and LIFRβ subunits), while type II OSMR consists of gp130 and OSMRβ subunits. This is significant as different subunits render mouse OSM incapable of activating the human OSM receptor. In addition, LIFR and OSMR subunits by themselves have low affinity to LIF and OSM cytokine binding, respectively, while the gp130 subunit does not bind to LIF or OSM, but it is required for high affinity binding to the complex. Note that the CT-1 and CNTF receptors contain a LIFRα subunit (Heinrich *et al.* 1998).

Upon activation of their respective cell surface receptor subunit (IL-6Rα, IL-11Rα, LIFR and OSMRβ), the gp130 co-receptor is recruited to form the receptor complex. These receptors do not possess intrinsic kinase activity; therefore, proximal association of the receptor subunits allow tyrosine kinase JAK1 (Janus kinase 1) to be recruited to gp130. Although gp130 is ubiquitously expressed, the phenotype of cells that respond to a certain IL-6 type cytokine is limited, since the expression of the α subunits is more restricted and tightly regulated. Soluble forms of the α subunits lacking the transmembrane and cytoplasmic domains have been identified for IL-6 (sIL-6Rα), IL-11 (sIL-11Rα), LIF (sLIFRα), OSM (sOSMRβ) and gp130 (sgp130). Soluble forms of these receptors are generated either by limited proteolysis (shedding) of membrane-bound receptors or by translation from an alternatively spliced mRNA. The

scenario becomes more complex as sIL-6Rα is agonistic and can initiate signalling in the absence of the membrane form of the receptor. In contrast, sgp130 possesses antagonistic activity. Identifying the signalling pathways of gp130 is essential in understanding the various effects of the IL-6 cytokine family on different cell types. Activated JAK1 phosphorylates membrane distal tyrosine residues of gp130 (Y^{767}, Y^{814}, Y^{905}, Y^{915}) to recruit STAT3 for activation, leading to a downstream JAK1/STAT3 signalling pathway (Figure 5). JAK2, and to a lesser extent TYK2 (tyrosine kinase 2), are also bound to gp130, LIFR and OSMR and activated along or in replacement of JAK1. Proximal association of receptor subunits also recruits and activates SHP2 (SH2-domain-containing tyrosine phosphatase) docking protein. It binds to Y^{759} of gp130 or Y^{974} of LIFR, leading to a MAPK or MEK (ERK1/2) signalling cascade. Thus, activation of IL-6 family cytokine receptors lead to two potential downstream signalling pathways. A number of in vitro studies have suggested that gp130-mediated activation of SHP-2 and ERK pathway results in generation of proliferative signals. In contrast, STAT3 activation appears critical for regulation of differentiation, apoptosis and gene transcription associated with terminally differentiated cells. These studies reveal tight reciprocal regulation between JAK-STAT and SHP2-ERK pathways, suggesting that balanced signalling from each pathway is critical for the generation of physiological responses to IL-6 family cytokines. Conversely, disturbance of this finely orchestrated signalling leads to pathological responses.

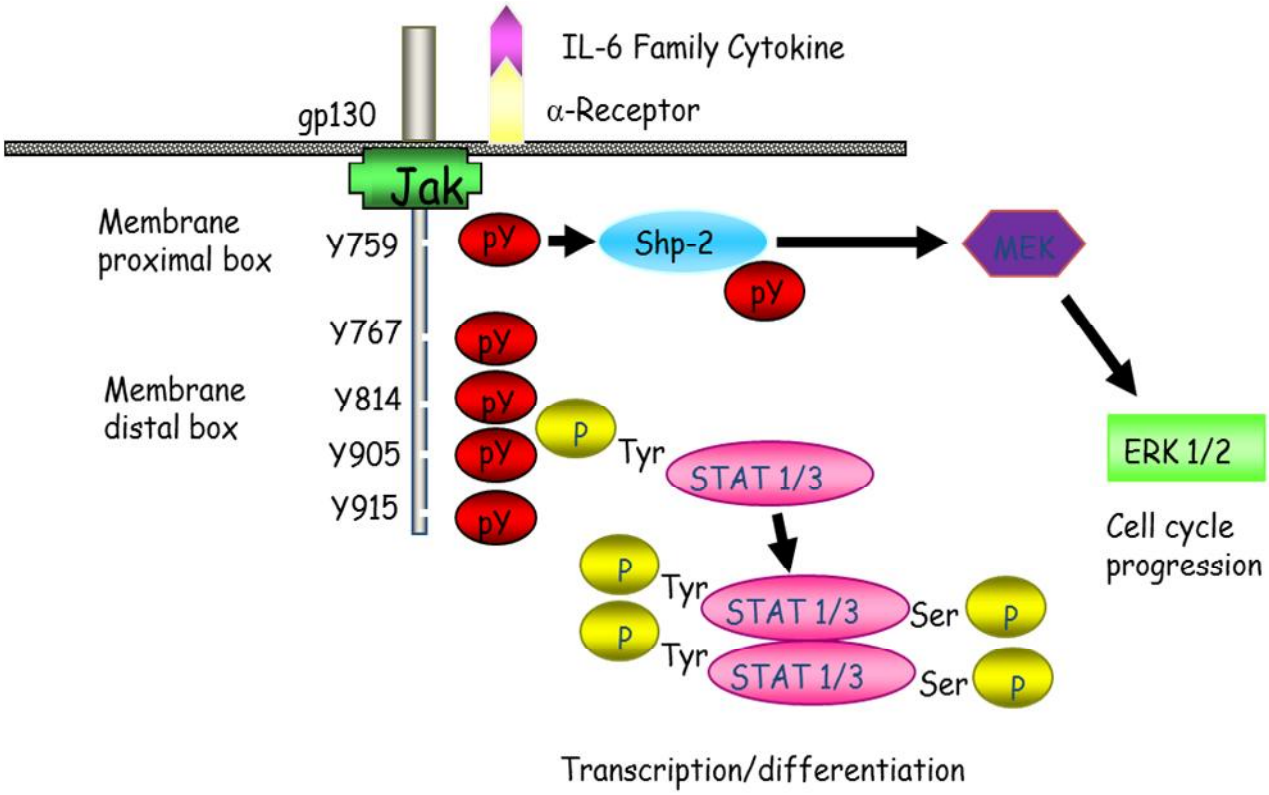

Figure 5. Downstream signalling of IL-6 Cytokine. Activation of the IL-6 receptor leads to phosphorylation of distal (Y767, Y814, Y905, Y915) and proximal (Y759) tyrosine residues of the gp130 receptor subunit and downstream JAK/STAT3 and Shp-2/MEK/ERK1/2 pathways, which lead to cell cycle progression and differentiation, respectively.

Several bodies of research highlighted the importance of IL-6 family members in inflammation and fibrosis. In a bleomycin-induced rat model of pulmonary fibrosis, IL-6 production and secretion by lung fibroblasts were elevated (Elias *et al*. 1990). Bleomycin is an antibiotic that has utility in some cancers. However, about 25% of patients taking this drug develop pulmonary fibrosis. Hence, it is a widely used model of pulmonary fibrosis (Karmouty-Quintana *et al.* 2007). It has also been shown clinically that IL-6 levels in the bronchoalveolar lavage fluid (BALF) of patients diagnosed with idiopathic pulmonary fibrosis were significantly increased compared to the control subjects (Jones *et al.* 1991). There is also a short nucleotide polymorphism (SNP) in Il-6 that associates with reduced lung capacity in IPF.

1.7. Signal-Transducer-and-Activator-of-Transcription-3 (STAT3)

STAT molecules have been extensively studied in IL-6 signalling. There are seven mammalian members of the STAT transcription factor family: STAT1, -2, -3, -4, -5a, -5b and 6 (Schaeffer *et al.* 1997). The domain structure, from N to C terminus, includes an oligomerization domain, coiled-coil domain, DNA binding domain, linker domain, SH2 (Src homology-2) domain and transactivation domain (Figure 6).

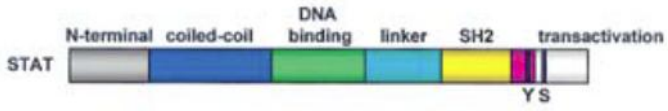

Figure 6. Schematic diagram of a STAT molecule. From N to C terminus, it contains a coiled-coil domain, DNA binding domain, linker domain, SH2 domain and transactivation domain. It contains two sites of phosphorylation, each for one of tyrosine or serine (Schaeffer *et al.* 1997).

All IL-6 family cytokines activate STAT3 via the common gp130 receptor subunit, and LIFR and OSMR subunits also activate STAT3, independently of gp130. STAT3 is found on locus 21.2 of chromosome 17 and is initially called an acute phase response factor. The STAT3 gene comprises of 24 exons and alternate splicing in exon 23 gives rise to two pleiotropic proteins: the α (770 amino acids, 93 kDa) and β (715 amino acids, 84 kDa) isoforms. STAT3β differs from STAT3α in a truncated 55 amino acids in the C terminal transactivation domain, but both isoforms are activated by the same cytokines and growth factors (Schaeffer *et al.* 1997). Activated STAT3β is more stable and has greater DNA binding specificity than STAT3α, but STAT3α, with an intact transactivation domain, has greater transcriptional activity. STAT3β lacks the serine phosphorylation site (Ser^{727}) within the carboxy-terminal transactivation domain,

but is still phosphorylated at Tyr^{705}. Knock-out mice have shown that Stat3β is not required for viability, whereas Stat3α-deficient mice die at birth (Maritano *et al*. 2004). Interestingly, expression of STAT3β can rescue the lethality associated with STAT3 knock-out. The same authors also showed that STAT3α has non-redundant roles in modulating IL-6 signaling and relative expression levels of Stat3α and Stat3β depend on cell type. Thus, for the most part, fibroblasts from $STAT3\alpha^{-/-}$ but not $STAT3\beta^{-/-}$ mice act like cells from $STAT3^{-/-}$ animals. In addition, in some inflammatory cells, STAT3α undergoes limited proteolysis to give rise to STAT3γ (72 kDa), which like STAT3β lacks the carboxyl-terminal portion of STAT3, and it is mostly found in neutrophils (Kato *et al.* 2004). STAT3δ (64 kDa) is another truncated version involved in granulocyte differentiation (Maritano *et al.* 2004).

STAT3 is expressed ubiquitously and constitutively. STAT3 is required for embryonic stem cell development as STAT3 deficient mouse embryos are lethal beyond embryonic day 7 (Takeda *et al.* 1997). However, constitutively active STAT3 is oncogenic with increased cell proliferation and decreased apoptosis and is associated with various cancers, including head and neck cancer, breast cancer, prostate cancer and glioblastoma (Turkson & Jove 2000). STAT3 can be rendered constitutively active by mutating alanine (A^{661}) and asparagine (N^{663}) to cysteine residues so that disulfide bonds can be formed between two STAT3 molecules, which enhances nuclear translocation.

1.8. STAT3 signalling following gp130 activation

Following phosphorylation of gp130 distal membrane tyrosine residues by JAK, monomeric STAT3 is recruited to the receptor complex and is activated by phosphorylation of Y^{705}, also by

JAK. This induces a conformational change in STAT3, allowing the transcription factor to expose its SH2 domain, where it homodimerizes or heterodimerizes with STAT1 (Schaeffer *et al.* 1997). The S^{727} residue can also be phosphorylated in the longer isoform, STAT3α, but its regulatory activity is ambiguous as there is evidence of both increased and decreased STAT3 activity upon its phosphorylation (Chung *et al.* 1997).

Once dimerized, a STAT3 nuclear localization sequence in the DNA binding domain that is important for interacting with importin-α5 is exposed and allows for nuclear import and DNA binding. Unphosphorylated STAT3 has limited ability to be translocated into the nucleus, but there is evidence that they are rapidly exported from the nucleus.

Transcription of STAT3 target genes is initiated via its transcription domain in the carboxyl-terminal end. STAT3 also interacts and recruits other transcription factors and co-activators to the promoters of its target genes (Snyder *et al.* 2007). As mentioned previously, STAT3 has been extensively studied in cancer research and STAT3 target genes are important in regulating cell proliferation and survival (e.g. cyclin D1, p53 and bcl-xl), cell migration and invasion (e.g. metalloproteinases-1, -2 and -9), angiogenesis (VEGF, basic fibroblast growth factor) and immune invasion (IP-10 and RANTES) (Huang *et al*. 2007). However, it has been recently shown that STAT3 regulates genes common to both wound healing and cancer (Dauer *et al.* 2005). For example, treatment with OSM in a mouse embryonic fibroblast cell line revealed STAT3 binding sites in the promoter of genes that include c-fos (involved in cell proliferation and differentiation to defense against invasion and cell damage), fgl2 (involved in fibrin deposition in blood coagulation) and SMAD9 (a downstream signalling molecule of TGFβ)

(Snyder *et al*. 2007).

As STAT3 is required for cell survival, but constitutive activation is pathological, its expression is tightly regulated by various mechanisms. For example, its activity is negatively regulated by endogenous protein tyrosine phosphatases SHP2 and protein inhibitor of activated STAT3 (PIAS3) (Heinrich *et al.* 2003). SHP2 dephosphorylates JAK, gp130 and STAT3, while PIAS inhibit STAT DNA binding (Heinrich *et al*. 2003). A target gene of STAT3 is suppressor of cytokine signalling-3 (SOCS3), which acts by a classical negative feedback mechanism by inhibiting JAK activation. There is evidence of STAT1 dephosphorylation within the nucleus by T-cell protein tyrosine phosphatase (Tc-PTP) (Heinrich *et al*. 2003), but whether this occurs for STAT3 is yet unknown.

1.9. STAT3 and fibrosis

While the specific role of STAT3 in fibrosis remains unclear, studies in liver, skin and kidney all point towards a regulatory role for STAT3 in the pathogenesis of fibrosis. However, these studies are contradictory with the results of some arguing for a protective role and others a pro-fibrotic role for STAT3. CCl4-induced liver fibrosis is increased in IL-6 deficient mice (Kovalovich *et al*. 2000). Furthermore, using the Cre-loxP system to knock-out gp130 signalling in hepatocytes (AlfpCre) or non-parenchymal cells (MxCre) on the effect of CCl4-induced liver fibrosis observed the evidence of disease progression in MxCre animals but not AlfpCre, suggesting that gp130-dependent signalling by non-parenchymal/immune cells protects these animals against progressive liver fibrosis (Streetz *et al.* 2003). In contrast, a number of studies

have reported a pro-fibrotic role for STAT3. Liver fibrosis is increased in liver-specific suppressor of cytokine signaling deficient ($SOCS3^{-/-}$) mice. This has been attributed to STAT3-mediated up-regulation of TGF (Ogata *et al.* 2006). It was also shown that increased STAT3 activation leads to liver fibrosis in mice in the presence of IL-6 (Hosui *et al.* 2009). In addition, STAT3-phosphorylation is enhanced in keloid scar tissue and inhibition of STAT3 activity in keloid fibroblasts reduces collagen production (Lim *et al.* 2006). A correlation has been made between STAT3 activation and renal function and injury, implicating STAT3 in the pathogenesis of renal disease. STAT3 knock-down mice are protected from induced kidney fibrosis (Lu *et al.* 2009). Inhibition of histone deacetylase (HDAC)-activated STAT3 has been shown to mediate renal interstitial fibroblast activation (Pang *et al.* 2009). These observations suggest that STAT3 may contribute to the progression of kidney disease. In addition, it has also been shown that STAT3 inhibitor, S3I-201, inhibits fibronectin expression in kidney fibrosis (Pang *et al*. 2010).

1.10. Previous research and proposed role of STAT3 in pulmonary fibrosis

In contrast to the data from other organs (see previous section), the role of STAT3 in pulmonary fibrosis has received far less attention. Data from our laboratory has previously shown that IL-6 inhibits proliferation of lung fibroblasts isolated from normal patients, while it increases proliferation in lung fibroblasts isolated from patients with IPF (Moodley, Scaffidi *et al.* 2003). Secondly, IL-6 enhances Fas induced apoptosis and increases expression of pro-apoptotic Bax protein in normal fibroblasts, but IL-6 inhibits Fas induced apoptosis and increases expression of anti-apoptotic protein Bcl-2 in IPF fibroblasts (Moodley, Misso *et al.* 2003). Thirdly, IL-6 and OSM mediate endothelin-1 induced hypertrophy of human airway smooth muscle cells via

activation of MEK/ERK and JAK/STAT3 (McWhinnie *et al*. 2007). Fourth, transfection of human lung fibroblasts with a lentiviral construct encoding a constitutively active form of STAT3 (called STAT3C) renders the morphology of the fibroblast to become more similar to that of a myofibroblast, aggregates of which are found in an IPF lung (Pechkovsky, MS submitted).

1.11. Hypotheses and Aims

1.11.1. Overarching hypothesis

Aberrant STAT3 activation significantly contributes to the pro-fibrotic function and phenotype of human lung fibroblasts. This manifests as increased proliferation and increased expression of ECM proteins (e.g. collagen, fibronectin).

1.11.2. Specific hypothesis 1

STAT3 activation by IL-6 family cytokines is an important inducer of pro-fibrotic lung fibroblast function and phenotype, which manifests as an increased proliferation and expression of collagen-1 and EDA-FN.

1.11.3. Aim 1

To determine whether STAT3 inhibition reduces IL-6 family cytokine induced collagen-1 and EDA-FN protein expression and cell proliferation in human lung fibroblasts.

1.11.4. Specific hypothesis 2

Differential cell proliferation upon IL-6 family cytokine stimulation in primary lung fibroblasts

isolated from normal patients and patients with IPF is due to divergent downstream signalling between JAK/STAT3 and MEK/ERK½ pathways.

1.11.5. Aim 2

To determine whether inhibition of STAT3 and MEK/ERK1/2 activity have differential effects on fibronectin protein expression and cell proliferation in human lung fibroblasts.

Chapter 2. Methods and Materials

2.1. Cytokines, growth factors and inhibitors

Recombinant human OSM and IL-6 were purchased from R&D Systems (Minneapolis, MN, U.S.A.). Recombinant human LIF was purchased from Sigma (Saint Louis, MO, U.S.A.). Recombinant human TGFβ1 was purchased from Pepro Tech Inc. (Rocky Hill, NJ, U.S.A.). STA-21 was purchased from Enzo Life Sciences (Plymouth Meeting, PA, U.S.A.). UO126 was purchased from Millipore (Temecula, CA, U.S.A.).

STA-21 is a small molecule inhibitor (306 Daltons) which was discovered via computer-based screening with the STAT3 protein crystal structure retrieved from Protein Data Bank (Song *et al.* 2005). The scientific name is deoxytetrangomycin, and it belongs to the class of angucycline antibiotics that is a naturally occurring microbial metabolite. It forms hydrogen bonds with three amino acid residues in the SH2 domain of STAT3 (R595, R609 and I634). STA-21 bound STAT3 is prevented from dimerization via their SH2 domains, which is a pre-requisite for nuclear translocation to transcribe its target genes. Subsequent evaluation of STA-21 in human breast cancer cell lines confirmed inhibition of STAT3-DNA binding activity and down-regulation of STAT3 dependent anti-apoptotic genes. UO126 is a selective and highly potent inhibitor of the Mitogen-Activated Protein Kinase (MAPK) cascade by inhibiting upstream MEK1 and MEK2. It inhibits both the active and inactive form of MEK. It was initially recognized as an activated-protein-1 (AP-1) antagonist (Duncia *et al.* 1998).

2.2. Cell culture

Human fetal lung (HFL) fibroblasts were obtained from American Type Culture Collection (ATCC, Rockville, MD, U.S.A.) and were used between passages 1 and 20. Cells were cultured in T-25 and/or T-75 tissue culture flasks with Dulbecco's Modified Eagle Medium (DMEM; Invitrogen, Burlington, Ontario) supplemented with 10% fetal bovine serum (FBS) and 50 units/ml penicillin and streptomycin. Primary human lung fibroblasts were established from explant cultures (Peckovksy *et al.* 2010) and were cultured in the same medium with additional supplement of 50 units/ml fungizone. Cells were kept in humidified atmosphere of 5% CO_2 in air at 37^{o}C. Medium was routinely changed every 3 to 4 days.

2.3. Optimizing cytokine induced protein expression in HFL fibroblasts – concentration and time dependence

The procedure for optimizing cytokine effects and protein expression is summarized in Figure 7. For determining the optimal concentrations, the fibroblasts were seeded into sterile, multi-well plastic, flat bottom plates (Becton Dickinson Labware, Franklin Lakes, NJ, U.S.A.) in medium containing 10% FBS and allowed to adhere overnight (16-18 hrs). At this time, cells were 80-90% confluent. IL-6 (1, 10, 100 ng/ml), OSM (10, 100 ng/ml) and LIF (10, 100 ng/ml) were added for 24 hrs, and cells were lysed with protein extraction buffer for determination of EDA-FN, collagen-1 and β-tubulin protein expression by western blotting. For determination of the optimal time required for ECM synthesis, IL-6 (100 ng/ml), OSM (2, 10 ng/ml) and LIF (10 ng/ml) were added for 24, 48 and 72 hrs.

a)

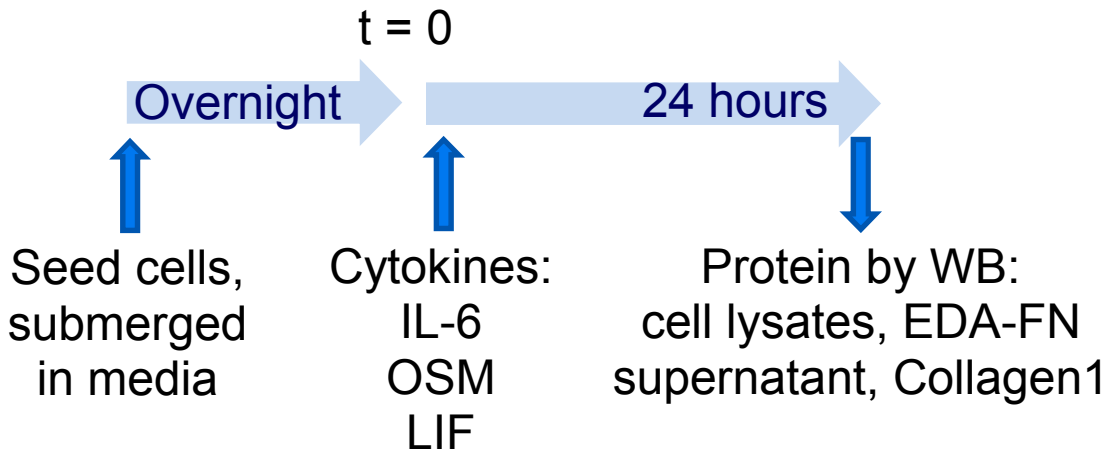

b)

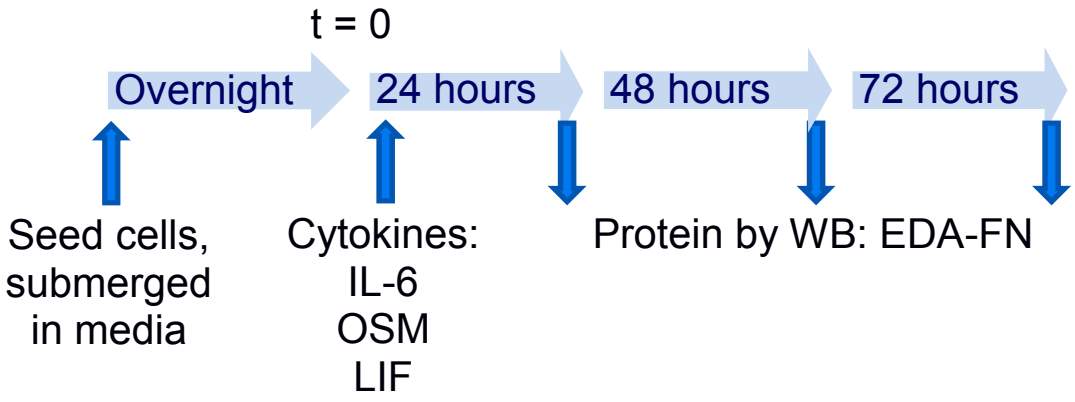

Figure 7. Timeline of cell culture in optimizing concentration and stimulation time of IL-6 family cytokines. IL-6, OSM and LIF were added at various concentrations for 24 hrs to determine the optimal concentration (a). The optimal concentrations were selected and added for 24, 48 and 72 hrs to determine the optimal stimulation time (b).

2.4. Optimizing OSM and STA-21 efficacy in fibroblasts

To determine whether 10 uM STA-21 and/or 2 ng/ml OSM are sufficient to remain active over 48 hrs, the need for repeated dosing was investigated. Fibroblasts were seeded at approximately 50,000 cells/well in 12-well plates in DMEM containing 10% FBS and allowed to adhere overnight. Single or double doses of STA-21 and OSM given every 24 hrs alone or in combination were compared. Prior to STA-21 addition, medium was changed to DMEM containing 1% FBS to reduce binding to STA-21. After 1 hr, OSM was added. At the end of the 48 hrs, protein was collected and quantified for STAT3 and pSTAT3 by western blotting.

2.5. Optimizing STA-21 incubation time in the presence of OSM

HFL fibroblasts were seeded in medium containing 10% FBS as mentioned above. The medium was changed to 1% FBS prior to addition of 10 uM STA-21 at 80-90% cell confluency. STA-21 was added 1, 6, 24 and 48 hrs prior to 2 ng/ml OSM stimulation for 48 hrs. STA-21 and OSM were re-added every 24 hrs (Figure 8). Protein expressions for STAT3, pSTAT3 and EDA-FN were analyzed by western blotting.

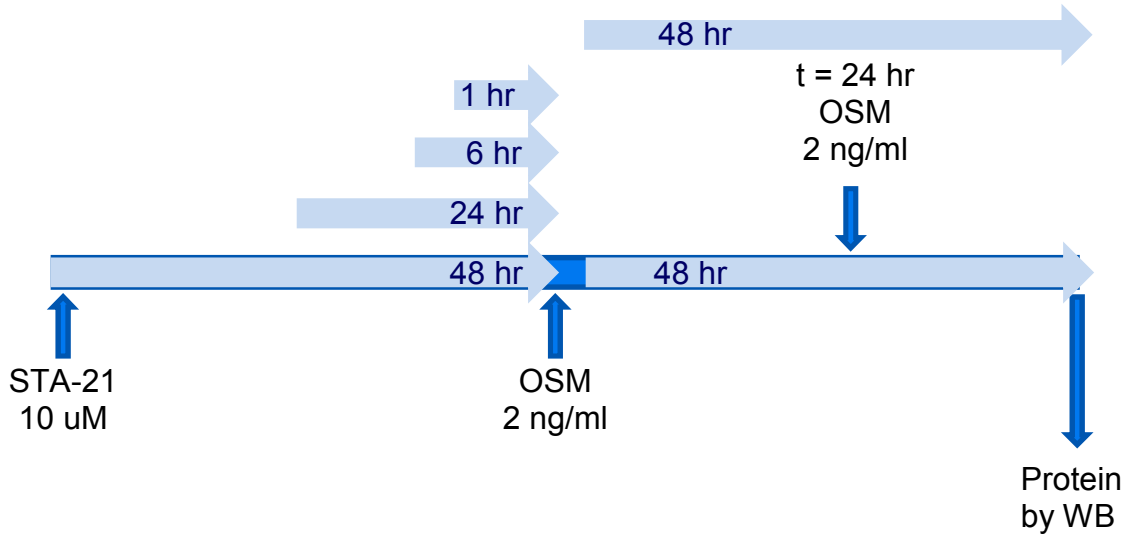

Figure 8. Timeline for determining the effect of OSM on protein expression of STAT3, pSTAT3 and EDA-FN in HFL fibroblasts with re-addition of STA-21 and OSM every 24 hrs as reinforcement. 10 uM STA-21 was added 1, 6, 24 and 48 hrs prior to stimulation with 2 ng/ml OSM. Whole cell lysates were collected after 48 hrs and proteins were analyzed by western blotting.

2.6. STA-21 treatment in primary fibroblasts

Fibroblasts were seeded at a density of 200,000 cells/well in 6-well plates overnight in DMEM containing 10% FBS. On the next day, the medium was changed to DMEM containing 1% FBS and 10 uM STA-21 was added. After one hr, fibroblasts were stimulated with 2 ng/ml OSM or 1 ng/ml TGFβ1 for an additional 48 hrs, after which proteins were collected and analyzed for EDA-FN, STAT3 and pSTAT3 by western blotting.

2.7. Optimization of STAT-3 siRNA

Approximately 50,000 fibroblasts were seeded in DMEM containing 10% FBS. ON-TARGET plus SMARTpool containing a combination of four STAT3 siRNA constructs (Thermo Scientific Dharmacon, Lafayette, CO, U.S.A.) at final concentrations 5, 10, 25, 50 and 100 nM were added

3 hrs post-seeding of fibroblasts. The control scrambled siRNA was always used at a final concentration of 25 nM (Qiagen, Mississauga, ON, Canada). The transfection reagent Hiperfect was added as a transfection reagent only control. Proteins were collected 48 hrs post siRNA addition, and the extent of STAT3 knock-down was evaluated by western blotting.

2.8. STAT3 siRNA with OSM and TGFβ1 stimulation in HFL and primary fibroblasts

STAT3 siRNA at final concentration of 25 nM was added 3 hrs post-seeding of both HFL and human primary lung fibroblasts. After 48 hrs, 2 ng/ml OSM or 1 ng/ml TGFβ1 was added for an additional 48 hrs. 2 ng/ml OSM was re-added after the first 24 hrs of stimulation in one condition. The scrambled control was used at a final concentration of 25 nM.

2.9. Western blotting

Protein expression in fibroblasts was assessed by Western blotting. The optimal time to collect protein depends on cell confluency as this affects STAT3 expression (Appendix). At the time of protein collection, cells were washed once with 1 x Phosphate buffered saline (PBS, HyClone, Utah, U.S.A.) and cell lysates were obtained by incubating cells with protein extraction buffer (1M Tris, NaCl, EDTA, EGTA, NaF, sodium pyrophosphate, sodium orthovanadate, Triton X-100, glycerol, 20% SDS, 10% sodium deoxycholate, pH 7.4), 0.1 uM PMSF, 1:100 phosphatase inhibitor cocktail and proteinase inhibitor cocktail 2 (Sigma, Saint Louis, MO, U.S.A.). Supernatant was also collected for analysis of secreted proteins, such as collagen-1. Protein content was determined using the DC Protein Assay (BioRad, Hercules, CA, U.S.A.). Equal amounts of protein (30-40 μg) were added to SDS loading buffer (20% SDS, glycerol, β-

mercaptoethanol, 0.1% bromophenol blue, 1M Tris, pH 6.8). Whole cell lysates, such as STAT3, EDA-FN and β-tubulin proteins, were denatured by boiling for 5 min prior to loading onto the gel. For measuring proteins in cell supernatant, β-mercaptoethanol and SDS were absent in the loading buffer. SeeBlue Plus2 prestained standard (Invitrogen, Burlington, Ontario, Canada) was used as a protein molecular weight ladder. Proteins were electrophoresed through 5% (collagen I) and 7.5% (STAT-3, EDA-FN) polyacrylamide gels and then transferred onto 0.45 μm nitrocellulose membranes (GE Water & Process Technologies, Minnetonka, MN, U.S.A.). Non-specific antibody binding was blocked by incubating membranes in 1xTBS/Casein (BioRad, Hercules, CA, U.S.A.) for 1 hr at room temperature. Membranes containing whole cell lysate proteins were probed with mouse monoclonal STAT-3 antibody 1:1000 (BD Transduction Laboratories, Mississauga, ON, Canada), rabbit polyclonal phospho-STAT3 (Tyr705) antibody 1:2000 (Cell Signaling, Pickering, ON, Canada) and mouse monoclonal EDA-FN antibody 1:1000 (Chemicon, Temecula, CA, U.S.A.) and incubated overnight at 4^{o}C. Mouse monoclonal β-tubulin antibody (Millipore, Temecula, CA, U.S.A.) 1:5000 was used as a loading control. Membranes containing supernatant proteins were probed with 1:5000 diluted rabbit polyclonal collagen-1 antibody (Abcam, Cambridge, MA, U.S.A.) and were incubated overnight at 4^{o}C. After repeated washes with 1xTBS containing 0.1% Tween, IRDye 800 conjugated anti-mouse goat IgG antibody (Rockland, Mississauga, ON, Canada) and IRDye 680 conjugated anti-rabbit goat IgG (Invitrogen, Eugene, Oregon, U.S.A.) antibody were diluted 1:5000 and added for 45 min to 2 hrs at room temperature. After further repeated washes with 1xTBS containing 0.1% Tween and one last wash with 1xTBS, the infrared signals were detected on the Odyssey Infrared Imaging System (LI-COR). Protein expression was quantified by densitometry of band intensity under the LI-COR system, as per manufacturer's instructions.

2.10. Cell proliferation

HFL fibroblasts were seeded in DMEM containing 10% FBS and 50 μg/ml penicillin and streptomycin at a density of 3000 cells/well in 96-well tissue culture plates and allowed to adhere overnight. The number of cells was counted using a Neubauer Haemocytometer (please refer to Figure 9 for time course of the experiment). Cells were quiesced by replacing the medium with 1% FBS overnight before being treated with OSM at 2 ng/ml for 48 hrs at 37^{o}C, 5% CO_2. In experiments that involved pharmacological inhibitors, 10 uM STA-21 or 10 uM UO126 were added 1 hr prior to the addition of OSM. Bromodeoxyuridine (BrdU) (1:500) was added 6 hrs prior to the end of the 48 hr OSM treatment. At the end of each incubation period, proliferation was assessed using a BrdU incorporation assay kit (Millipore, Temecula, CA, U.S.A.), according to the manufacturer's instructions. Briefly, following fixation of the cells and partial denaturation of doubled stranded DNA, monoclonal mouse BrdU antibody 1:200 was added and allowed to incubate overnight at 4^{o}C. Horse radish peroxidase conjugated goat anti-mouse IgG 1:2000 was filtered through a 0.2 μm syringe and then added to incubate for 30 min at room temperature. TMB (3,3',5,5'-tetramethylbenzidine) substrate was added for an additional 30 min at room temperature in the dark, followed by quenching with an acidic stop solution that transformed the blue oxidized product of TMB into a yellow product, which was detected at a single wavelength of 450 nm by a RLT Rainbow spectrophotometer microplate reader.

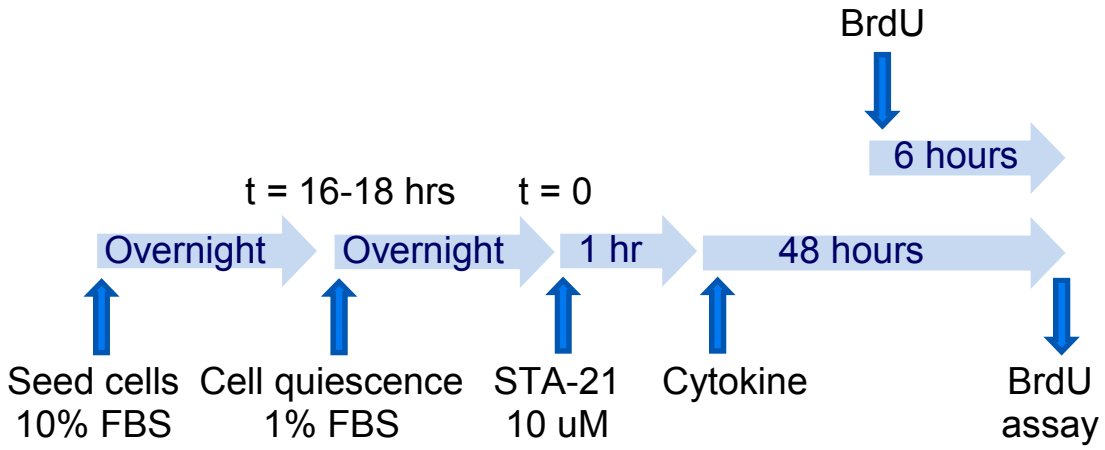

Figure 9. Timeline for quantifying cell proliferation by BrdU incorporation. HFL fibroblasts were seeded at 10% FBS for maximal growth, after which they were quiesced in 1% FBS to align cell cycle.

2.11. Immunofluorescence staining and confocal microscopy

Fibroblasts were seeded at a density of 8000 cells/well in DMEM containing 10% FBS and 50 µg/ml penicillin and streptomycin in 8-well tissue culture chamber slide (Lab-Tek, Rochester, NY, U.S.A.) and allowed to adhere overnight. Medium was changed to 1% FBS prior to addition of STA-21 (10 uM) or DMSO (vehicle control) for 48 hrs, after which 2 ng/ml OSM was added for either 30 min or 1 hr. The medium was removed and cells were washed 3 times in 1 x PBS (HyClone, Utah, U.S.A.). Fibroblasts were then fixed onto the culture slide with 100% methanol for 20 min at -20^{o}C. After 3 x 5 minute PBS washes, 5% goat serum (in PBS) was added for 60 min at room temperature to block non-specific binding of antibody, followed by additional 3 x 5 min PBS washes. Fixed cells were then incubated with either rabbit polyclonal phospho-STAT3 (Tyr705) antibody (Cell Signaling, Pickering, ON, Canada) diluted 1:100 in PBS containing 2.5% goat serum or PBS containing 2.5% goat serum (negative control) overnight at 4^{o}C. After 3 x 5 minute washes with PBS, goat anti-rabbit IgG Alexa Fluor 594 diluted 1:200 in 1 x PBS containing 2.5% goat serum was added for incubation of 2 hrs at room

temperature. During the last 15 minutes, 4',6-diamidino-2-phenylindole (DAPI, Sigma, Saint Louis, MO, U.S.A.) in PBS was added. After the last 3 x 5 min washes with PBS, fluorescence images were acquired using a Leica AOBS SP2 laser scanning confocal microscope (Leica, Heidelberg, Germany) with Zeiss LSM 510 software, version 3.2. Three-dimensional reconstruction and iterative deconvolution were applied to these images before classification of fluorescent pixels to perform comparative measurements for each of the two fluorescent markers using Volocity software (Improvision, Lexington, M.A.).

2.12. Statistical analysis

Each experiment was performed in duplicate and each set of experiments were repeated at least three times unless otherwise stated. Data are expressed as mean ± standard error of the mean. Statistical comparisons of mean data were performed using one-way ANOVA with post-hoc Bonferonni correction for multiple comparisons and a p-value of <0.05 was considered significant. For immunofluorescence analysis, Pearson's correlation was used. This represents the degree of overlap of two different fluorescent colors, with unity representing 100% overlap.

Chapter 3. Results

3.1. Optimization of IL-6 family cytokine concentration and time

IL-6 (1, 10, 100 ng/ml), OSM (10, 100 ng/ml) and LIF (10, 100 ng/ml) produced concentration dependent increase in EDA-FN protein expression compared to untreated control after 24 hrs of treatment in HFL fibroblasts (Figure 10a). Increasing concentrations of IL-6 increased EDA-FN dose-dependently to a maximum of 110% above the unstimulated cells. OSM and LIF produced similar effects on EDA-FN at the selected concentrations, with more variability seen for OSM. In contrast to EDA-FN, none of the cytokines induced significant collagen-1 protein expression compared to the untreated control (Figure 10b).

OSM (2, 10 ng/ml), IL-6 (100 ng/ml) and LIF (10 ng/ml) produced time-dependent increases in EDA-FN protein expression compared to the untreated control. After 24 hrs, OSM (2, 10 ng/ml) increased EDA-FN to a maximum of 150% compared to the 24 hr untreated control (Figure 11a). After 48 or 72 hrs, 2 ng/ml OSM increased EDA-FN, but 10 ng/ml OSM produced little or no effect compared to untreated control at their respective times. Both 100 ng/ml IL-6 and 10 ng/ml LIF increased EDA-FN approximately 50% above the untreated 24 hr control. We have previously shown that a single treatment of STA-21 (10 uM) in HFL fibroblasts is an effective treatment since it decreased STAT3 protein expression at 24 and 72 hrs (Appendix).

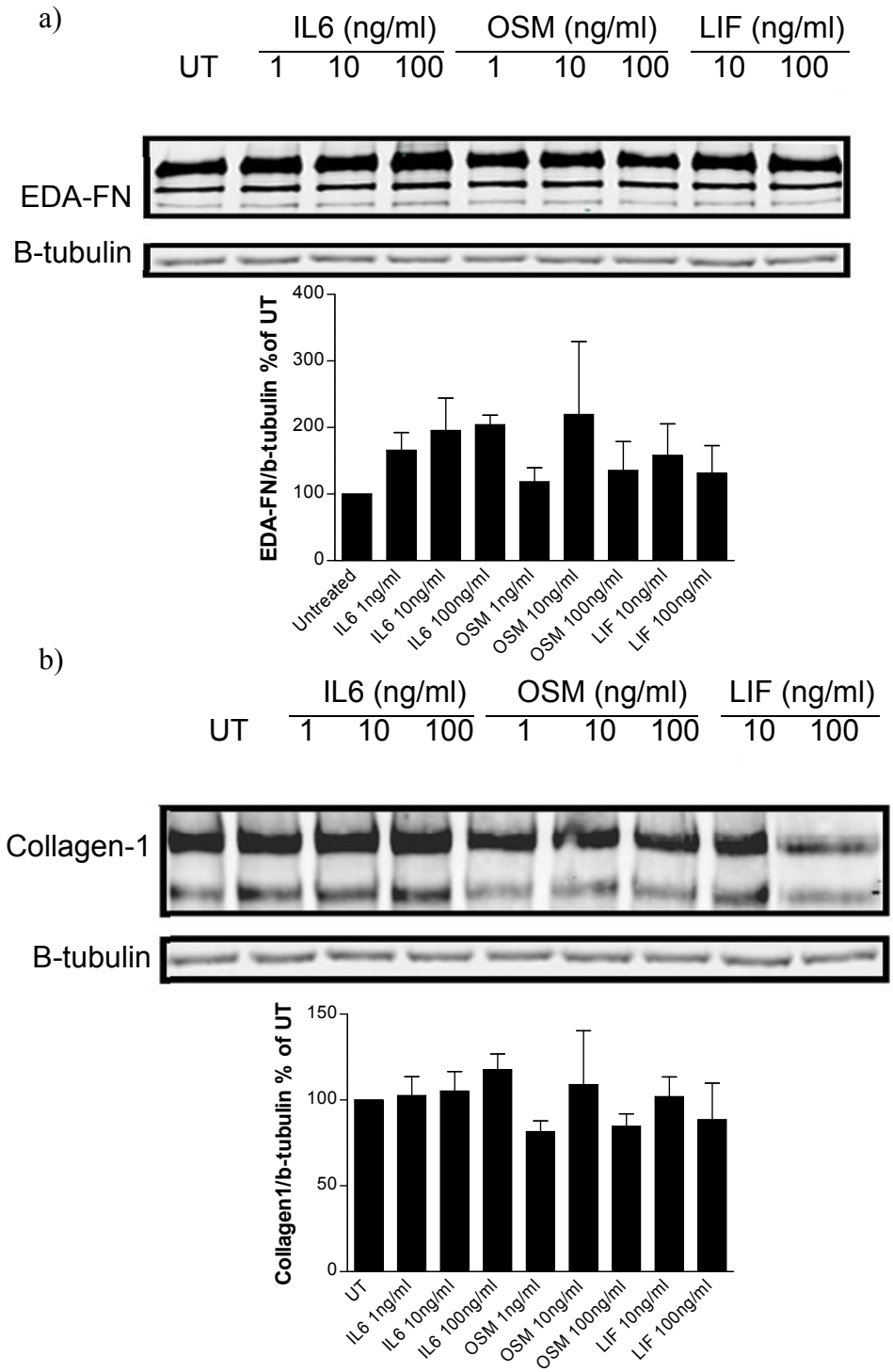

Figure 10. Concentration dependence of IL-6 family cytokines on EDA-FN and collagen-1 protein expression in HFL fibroblasts. Proteins were harvested 24 hrs post cytokine treatment. Protein expression is normalized to β-tubulin and expressed as percentage of untreated control. Despite statistical insignificance, there are trends of increasing EDA-FN protein with IL-6 concentration and peak EDA-FN at 10 ng/ml OSM and LIF (a). Collagen-1 expression is unaffected by IL-6 family cytokines (b). N=3.

a)

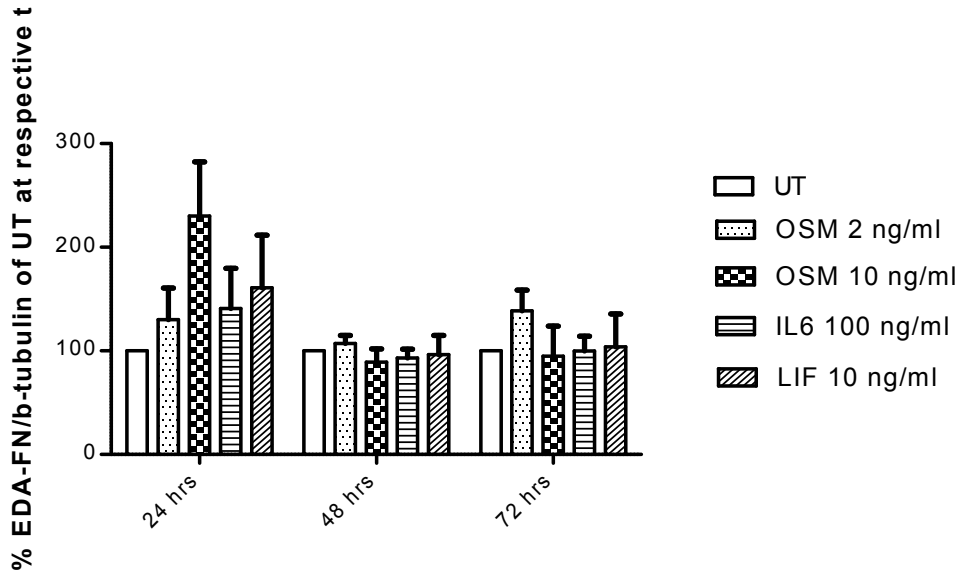

b)

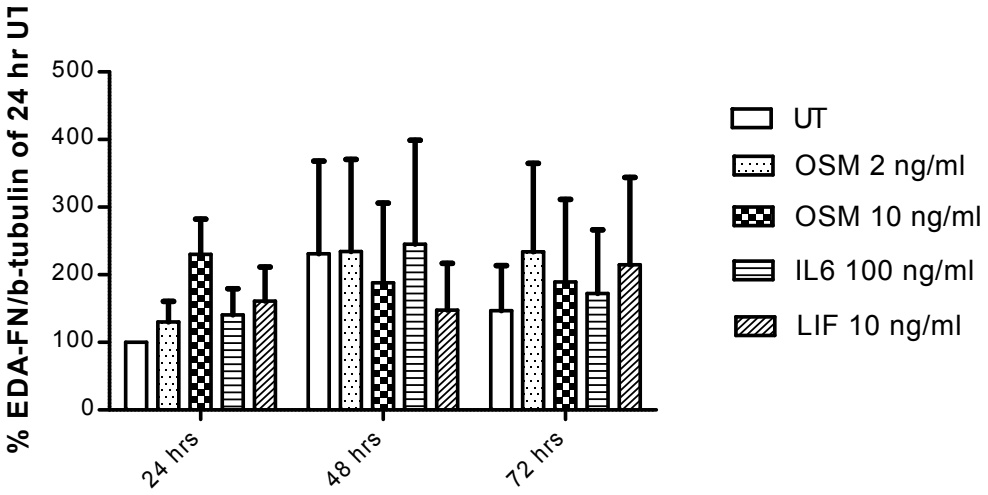

Figure 11. Time dependence of IL-6 family cytokines on EDA-FN protein expression in HFL fibroblasts. Proteins were harvested 24, 48 and 72 hrs post cytokine treatment. EDA-FN protein expression is normalized to β-tubulin and expressed as percentage of a) untreated control at their respective time of harvesting proteins or b) untreated control at 24 hrs. Statistical insignificance with $p>0.05$, N=4.

3.2. Immunofluorescence and confocal microscopy

STA-21 is proposed to prevent pSTAT3 translocation into the nucleus. Immunofluorescence staining for pSTAT3 and the nucleus can provide an image of analysis of pSTAT3 localization. Immunofluorescence staining of DNA in HFL fibroblasts revealed the nucleus in blue (Figure 12). In the absence of OSM stimulation, there was little or no pSTAT3 present. A series of controls were used, including omission of primary antibody, unstimulated cells, drug vehicle, DMSO (0.05% dimethyl sulfoxide), or drug only (10 uM STA-21). Stimulation with OSM (2 ng/ml) for 30 min increased intracellular pSTAT3. Expression of pSTAT3 was dispersed throughout the fibroblast and outlined its morphology. Pretreatment with STA-21 followed by OSM for 30 min did not produce observable differences compared to OSM stimulation alone. Indeed, the degree of fluorescence overlap as quantified by the Pearson's correlation, for OSM only and OSM with STA-21 were 0.520 and 0.574, respectively. However, stimulation with OSM (2 ng/ml) for 1 hr increased pSTAT3 fluorescence in the nucleus, producing a Pearson's correlation value of 0.621, and pSTAT3 no longer outlined the morphology of the fibroblast. Pretreatment with STA-21 followed by OSM for 1 hr decreased pSTAT3 in the nucleus, with a Pearson's correlation value of 0.506, compared to OSM (1 hr) alone. Appreciable expression of pSTAT3 was observed outside the nucleus.

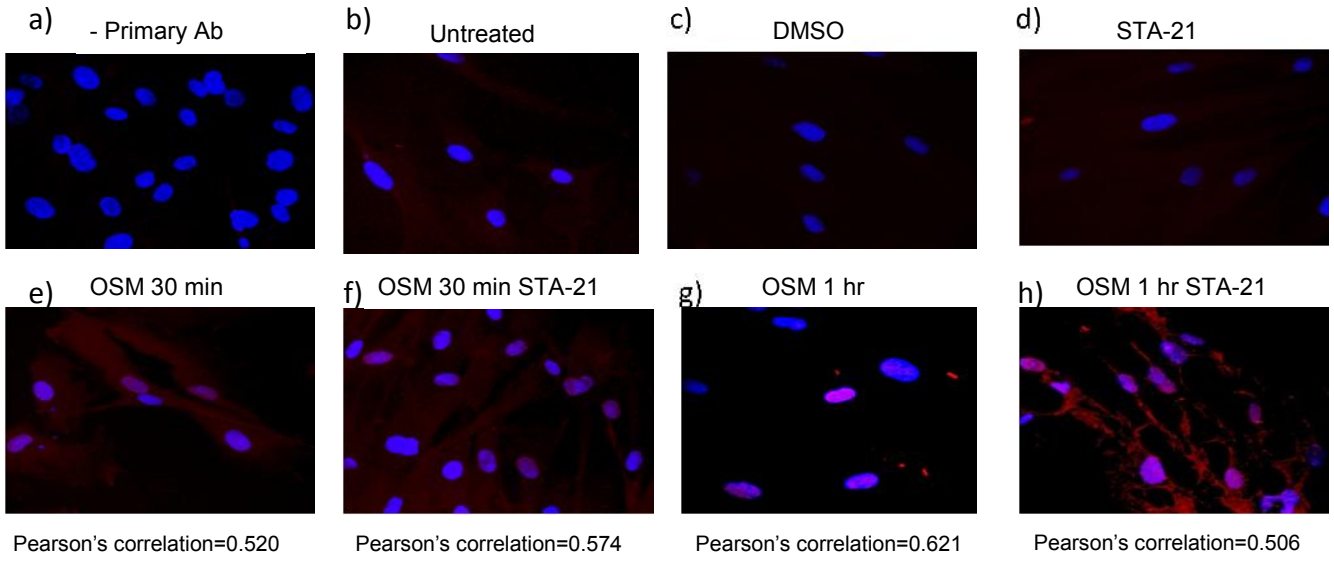

Figure 12. Immunofluorescence staining of HFL fibroblasts. The nucleus is represented by staining of DNA in blue by DAPI, and pSTAT3 is represented in red by staining with Alexa Fluor 594. DAPI only (a), untreated (b), drug vehicle 0.05% DMSO (c) and 10 uM STA-21 (d) showed only the nucleus. Stimulation with 2 ng/ml OSM for 30 min (e), OSM for 30 min plus 48 hrs pretreatment with STA-21 (f), OSM for 1 hr (g) and OSM for 1 hr plus 48 hrs pretreatment with STA-21 (h) showed both nucleus and pSTAT3. The degree of overlap between the blue and red fluorescence is quantified by the Pearson's correlation, and represents cytoplasmic or nuclear pSTAT3. N=2.

3.3. Maintaining STA-21 and OSM activity

Stimulation with OSM (2 ng/ml) for 48 hrs increased STAT3 activity in HFL fibroblasts compared to the untreated control, but the increase was statistically significant only when OSM activity was re-added after the first 24 hrs (Figure 13a,b). A single treatment of STA-21given 1 hr prior to OSM treatment inhibited total and fractional pSTAT3 induced by a repeated application of OSM. However, the inhibitory effects of double STA-21 treatments on double dosed OSM induced STAT3 activity was more pronounced. In addition, STA-21 (10 uM) decreased STAT3 expression, and as a result, total and fractional pSTAT3 also decreased, but the decreases were independent of STA-21 re-addition at 24 hrs. DMSO (0.05%) had no effect on STAT3 expression and activity.

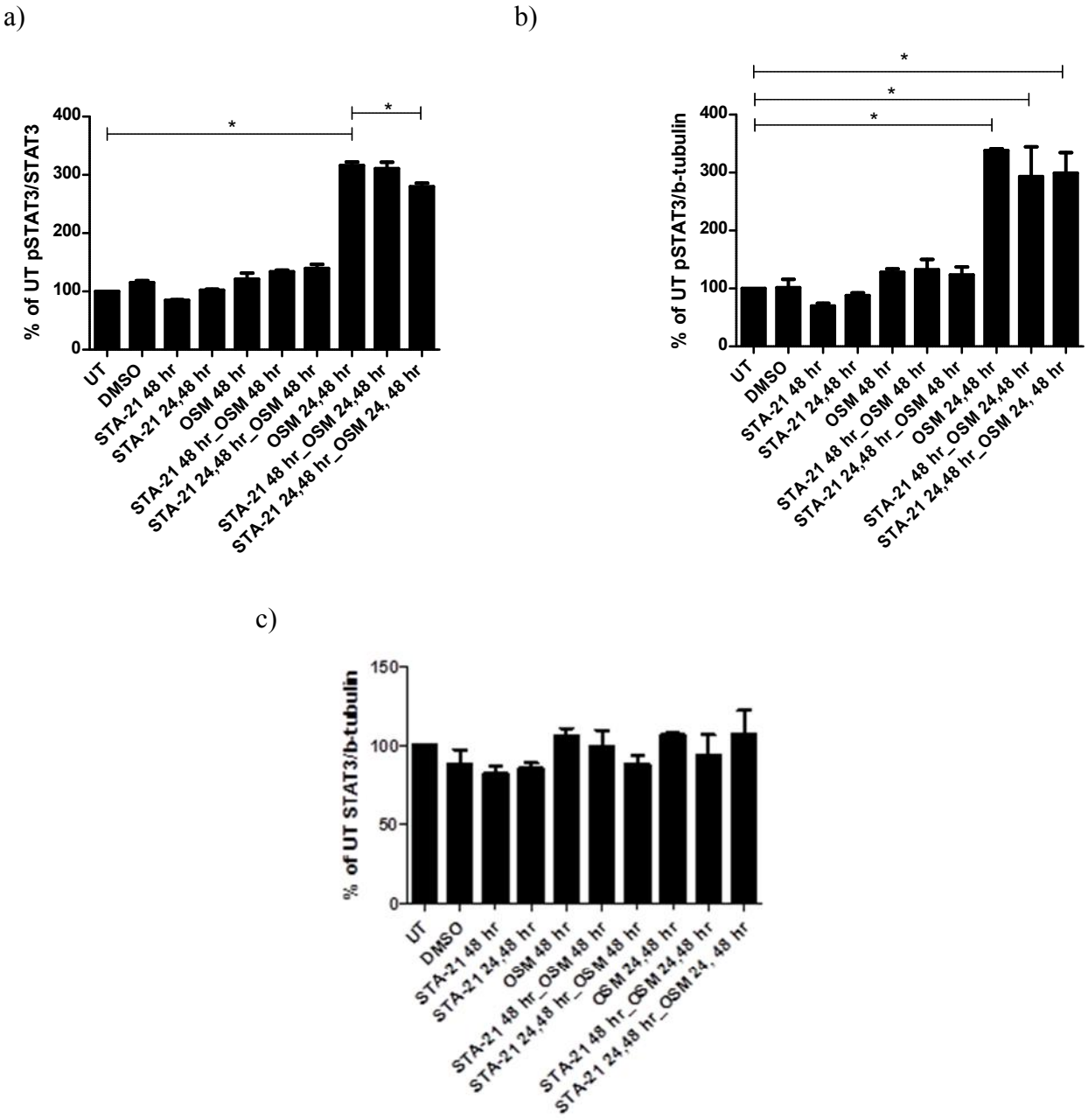

Figure 13. Effects of re-adding STA-21 and OSM on STAT3 protein expression and activity in HFL fibroblasts. OSM was added for 48 hrs, with or without re-addition of OSM and/or STA-21 after the first 24 hrs of OSM stimulation. Proteins were measured for fractional pSTAT3 (a), total pSTAT3 (b) and STAT3 (c). Data is normalized to β-tubulin SDS-PAGE loading control. Statistical significance indicated (*) with $p<0.05$, N=2.

3.4. Time dependent inhibition of EDA-FN expression by STA-21

A low level of EDA-FN was expressed in HFL fibroblasts in the absence of any exogenous stimulation (Figure 14a). OSM (2 ng/ml) stimulation at 24 and 48 hrs produced a 100% increase in EDA-FN protein compared to the untreated control (Figure 14b). STA-21 (10 uM), re-added every 24 hrs, produced time-dependent inhibition of OSM induced EDA-FN protein expression. Pretreatment with STA-21 for 1 hr prior to OSM stimulation resulted in the greatest degree of inhibition (approximately 90% inhibition of EDA-FN compared to OSM only). Pre-incubation with STA-21 for 6 hrs (approximately 75% inhibition) and 24 hrs (approximately 60-70% inhibition) were less effective. Pretreatment of STA-21 for 48 hrs did not inhibit OSM induced EDA-FN protein expression.

a)

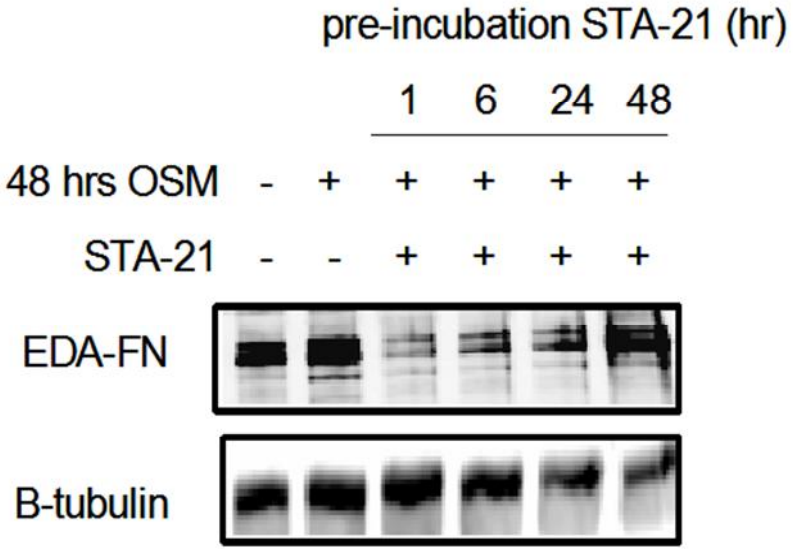

b)

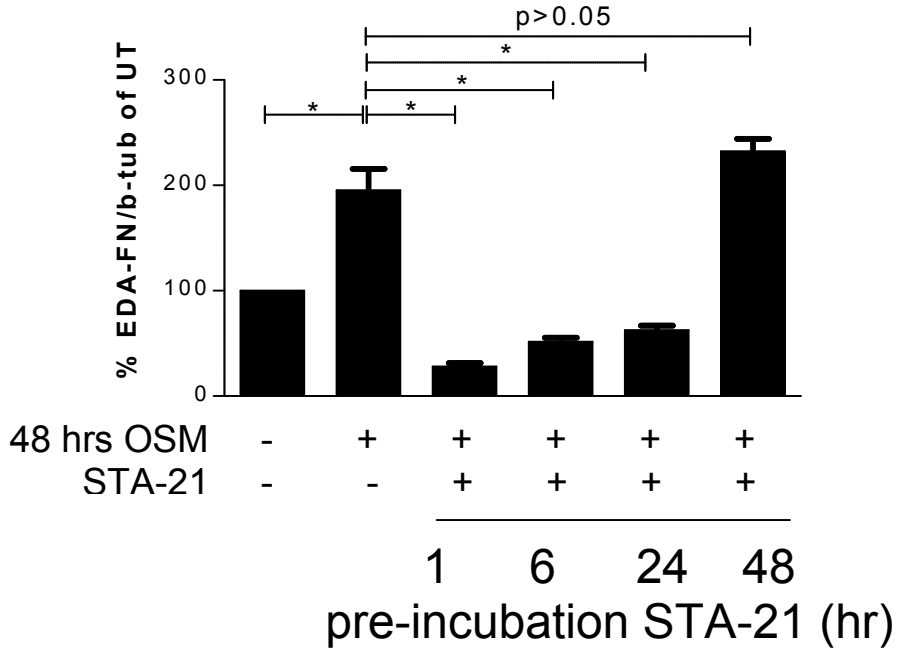

Figure 14. STA-21 time-dependently inhibited OSM-induced EDA-FN protein expression in HFL fibroblasts. STA-21 (10 uM) was added 1, 6, 24 and 48 hrs prior to stimulation with OSM (2 ng/ml) for an additional 48 hrs (re-added after the first 24 hrs). Protein expression is normalized to β-tubulin (loading control) and expressed as percentage of untreated control. Statistical significance indicated (*) with $p<0.05$, N=3.

As was seen for EDA-FN, STAT3 was also expressed in HFL fibroblasts in the absence of STA-21 treatment and OSM stimulation, but there was minimal pSTAT3 (Figure 15a). Stimulation with OSM increased both total STAT3 and pSTAT3 approximately 300% more compared to the untreated control (Figures 15a and 15b i, ii). Exposure to STA-21 inhibited OSM induced STAT3 and pSTAT3 expression (Figures 15b ii and iii).

a)

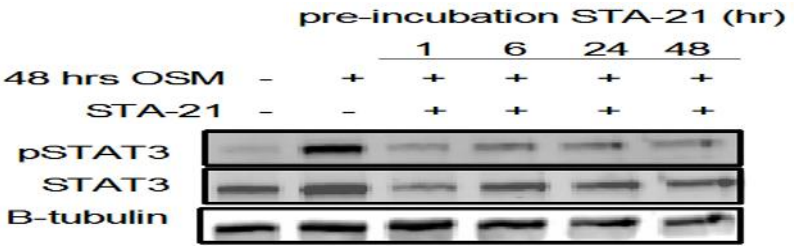

b) (i)

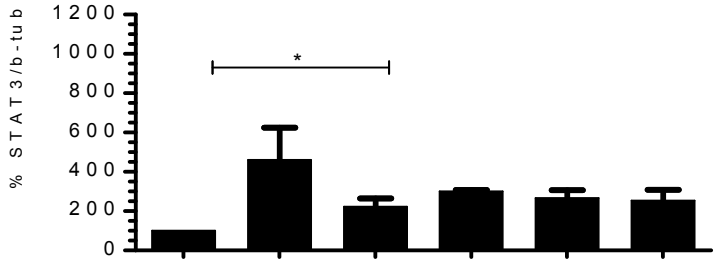

(ii)

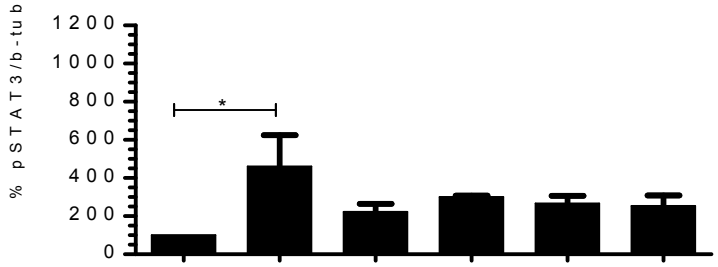

(iii)

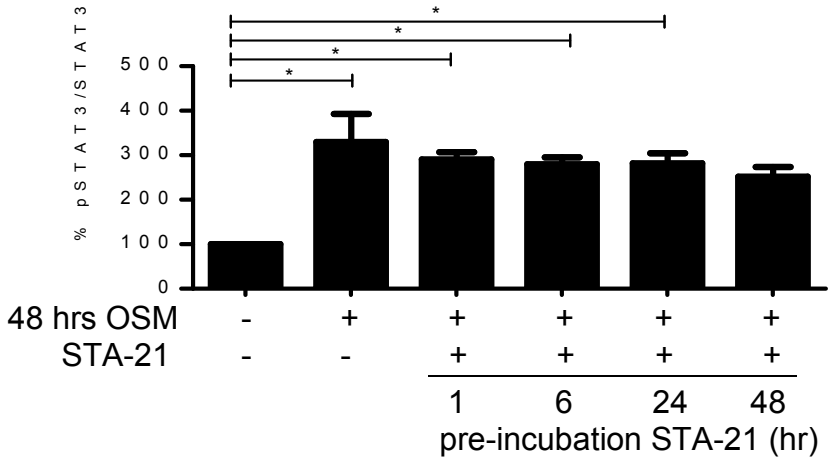

Figure 15. Time-independent STA-21 *inhibition of OSM induced STAT3 protein* expression and activation in HFL fibroblasts. STA-21 (10 uM) was added 1, 6, 24 and 48 hrs prior to stimulation with OSM (2 ng/ml) for an additional 48 hrs (both re-added after the first 24 hrs). Western blot of STAT3 and pSTAT3 protein (a) was quantified by densitometry by normalizing total STAT3 and pSTAT3 protein to β-tubulin, the loading control (b(i), b(ii)) or by normalizing pSTAT3 to STAT3 (b(iii)) and expressed as percentage of untreated control. Statistical significance indicated (*) with $p<0.05$, N=3.

3.5. STAT3 siRNA optimization

Given that small molecule inhibitors may have some off-target effects, we used an alternative approach - STAT3 siRNA as an adjunct to STA-21 to inhibit STAT3 activity. A pool of four STAT3 siRNAs produced concentration independent knockdown of STAT3 protein (Figure 16). Total cellular STAT3 protein decreased to approximately 50% of the untreated control. In contrast, transfection reagent and scrambled STAT3 siRNA controls produced little or no STAT3 knock-down activity.

a)

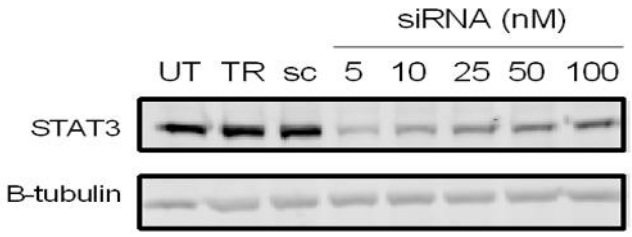

b)

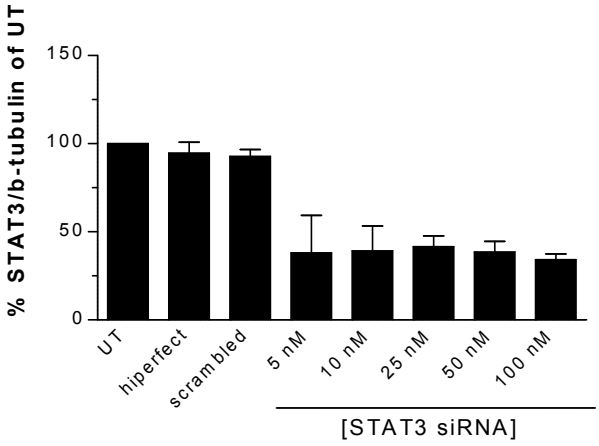

Figure 16. Concentration independent knockdown of STAT3 protein expression by STAT3 siRNA in HFL fibroblasts. A pool of four siRNA constructs were added with final concentrations 5, 10, 25, 50 and 100 nM for 48 hrs in 10% FBS and produced more than 50% knock-down of STAT3 protein expression compared to the scrambled control containing a scrambled STAT3 knockdown sequence. The scrambled siRNA (sc, 25 nM), transfection reagent (TR, hiperfect) and untreated control (UT) showed similar levels of STAT3 expression. STAT3 expression was performed by Western blot analysis (a), which was quantified by densitometry by normalizing STAT3 to loading control β-tubulin (b). STAT3 protein expression was further normalized to the UT control, which was set as 100%. Values represent the average of two experiments. N=2.

3.6. The effect of STAT3 siRNA on OSM stimulation in HFL fibroblasts

STAT3 siRNA (25 nM) knocked-down STAT3 protein expression approximately 90% of the untreated control after 48 hrs in HFL fibroblasts (Figure 17a). The transfection reagent and scrambled control had no effect on STAT3 expression. OSM (2 ng/ml) increased STAT3 expression more than 100% of the untreated control. STAT3 siRNA significantly inhibited OSM induced increase in STAT3 expression.

OSM (2 ng/ml) significantly increased pSTAT3 (Figure 17b). STAT3 siRNA knock-down of STAT3 protein expression resulted in decreased total pSTAT3 and significantly inhibited OSM induced increase in pSTAT3.

The increase in pSTAT3 after OSM (2ng/ml) corresponded with nearly 200% increase in EDA-FN expression (Figure 17d). STAT3 siRNA knock-down of STAT3 and pSTAT3 resulted in decreased EDA-FN after OSM, which was seen with STA-21. The transfection reagent and had no effect on pSTAT3 and EDA-FN. The scrambled sequence increased pSTAT3, which resulted in increased EDA-FN.

Double stimulation with OSM had no effect on STAT3 expression, but sustained the increase in total and fractional pSTAT3 (Figure 17c). Yet EDA-FN was similar to the untreated control.

TGFβ1 (1 ng/ml) had no effect on STAT3 expression and activity. TGFβ1 alone increased EDA-FN expression by approximately 300% more than the untreated control. STAT3 siRNA had no effect on TGFβ1 induced EDA-FN expression.

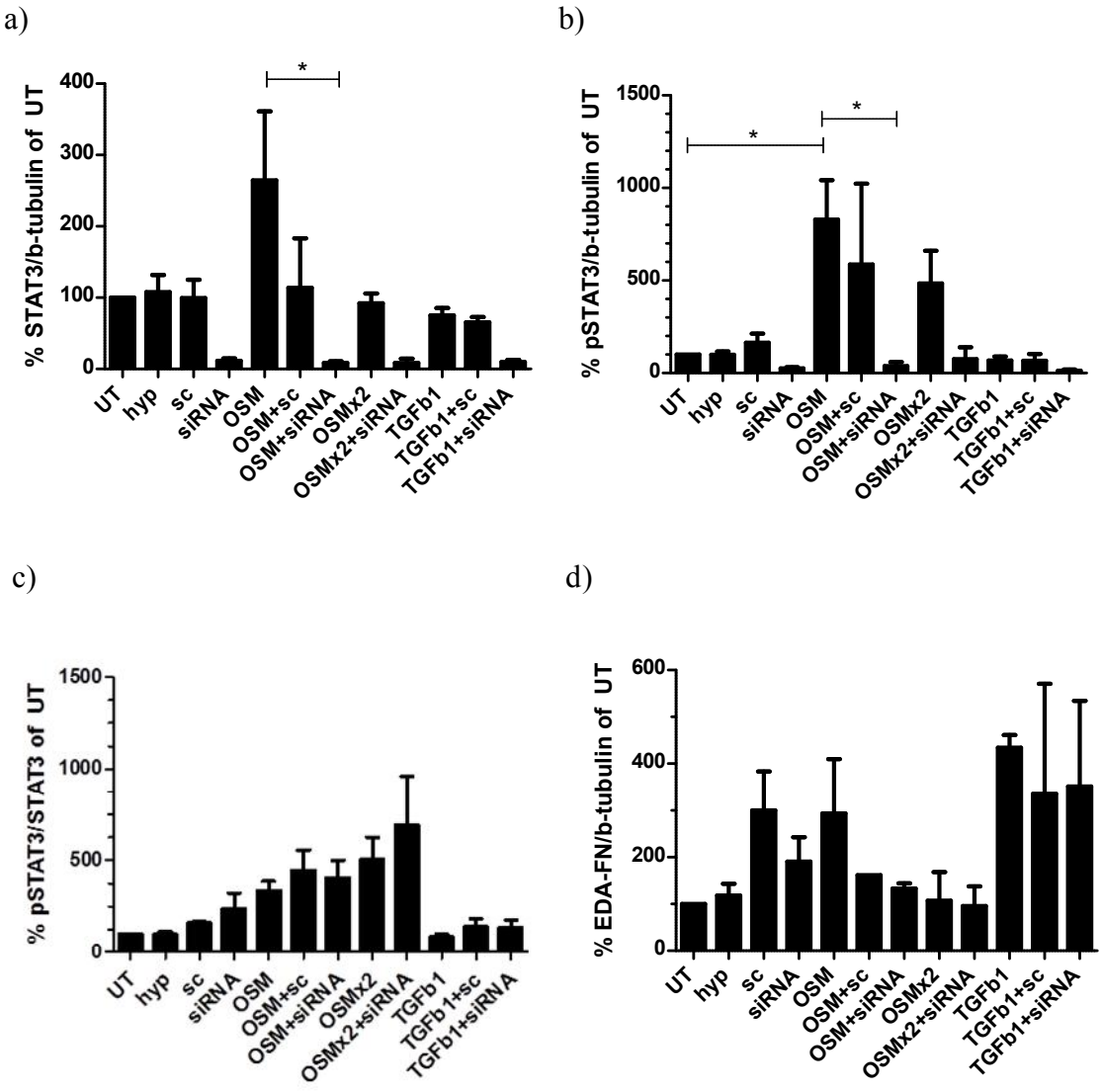

Figure 17. Effect of STAT3 knockdown on STAT3 activity and EDA-FN protein expression with OSM stimulation in HFL fibroblasts. A pool of four STAT3 siRNAs (25 nM) was added for 48 hrs, followed by OSM (2 ng/ml) or TGFβ1 (1 ng/ml) for an additional 48 hrs. OSM was either re-added or not after the first 24 hrs. OSM increased STAT3 expression (a) and activity (b, c) and EDA-FN (d), and STAT3 knockdown by siRNA significantly inhibited OSM induced STAT3 and total pSTAT3, but did not inhibit OSM induced EDA-FN. Re-addition of OSM increased fractional pSTAT3, but had no effect on EDA-FN. Statistical significance with one way ANOVA and Bonferroni post-hoc test, $p<0.05$, N=3.

3.7. Effect of STA-21 in primary human fibroblasts

Given that fetal and adult fibroblasts show differences in wound healing capacity, we next sought to examine the effect of STAT3 manipulation on EDA-FN expression. As was seen for HFL fibroblasts, basal EDA-FN protein was expressed in normal primary fibroblasts (Figure 18). However, in contrast to HFL fibroblasts, treatment with OSM (2 ng/ml) alone (or STA-21 (10 uM) alone) for 48 hrs had no significant effect on EDA-FN expression. This was not a generalized phenomenon of unresponsive cells since TGFβ1 (1 ng/ml) increased EDA-FN expression 200% more than the untreated control. However, STA-21 had no effect on TGFβ1 induced EDA-FN expression.

As was seen for EDA-FN, OSM had no effect on collagen-1 expression (Figure 19). Accordingly, STA-21 did not modify the responses to OSM. As expected, TGFβ1 (1 ng/ml) increased collagen-1 by nearly 100% compared to the untreated control, but STA-21 had no significant effect on this response.

As in HFL fibroblasts, OSM increased total and fractional pSTAT3 (nearly 500%) in primary fibroblasts, but in contrast, OSM did not change STAT3 expression (Figure 20). Surprisingly, STA-21 did not inhibit OSM induced increase in total and fractional pSTAT3. TGFβ1 (1 ng/ml) had no effect on STAT3 expression.

In an attempt to determine whether diseased cells would behave differently, we investigated the effects of OSM and STA-21 in a small number of fibroblast cultures from asthmatics (Figure

21). The effects of STA-21, OSM and TGFβ1 on EDA-FN protein expression in primary asthmatic bronchial fibroblasts were similar to those in primary normal bronchial fibroblasts.

a)

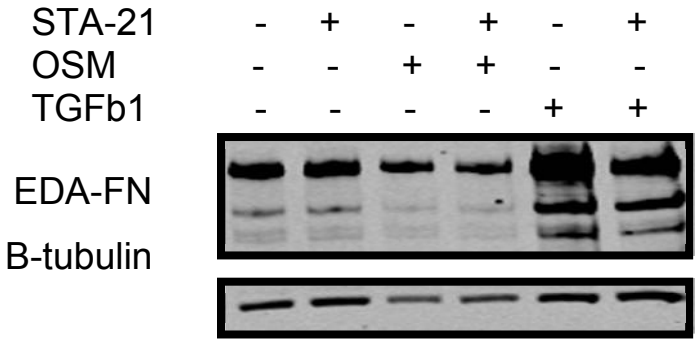

b)

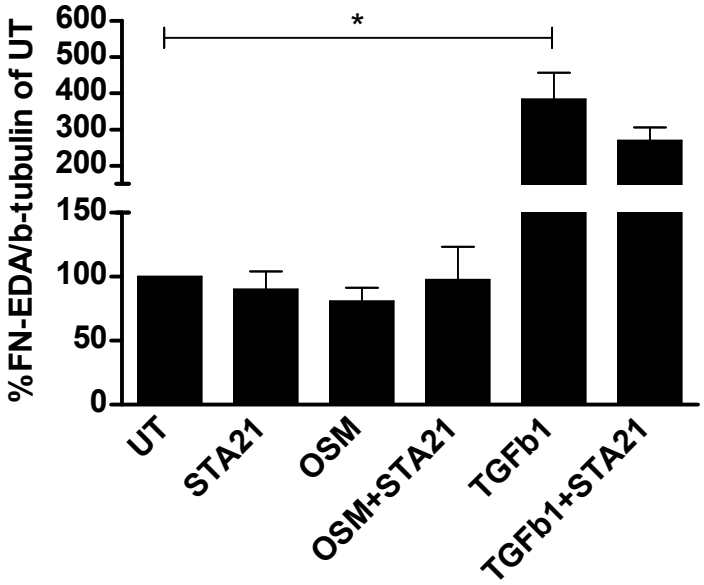

Figure 18. Effect of OSM and STA-21 on EDA-FN protein expression in normal primary fibroblasts. Fibroblasts were treated with STA-21 (10 uM) only, OSM (2 ng/ml) only, STA-21 and OSM, TGFβ1 (1 ng/ml) only, TGFβ1 and STA-21 or left untreated. TGFβ1 represents a profibrotic positive control. STA-21 treatment was one hr prior to OSM or TGFβ1 stimulation for an additional 48 hrs. The western blot analysis (a) was quantified by densitometry with β-tubulin as a loading control. EDA-FN expression in the untreated condition is set as 100%, and data is normalized to this value. Statistically significant (*) with one way ANOVA with Bonferonni post-hoc, $p<0.05$, N=3.

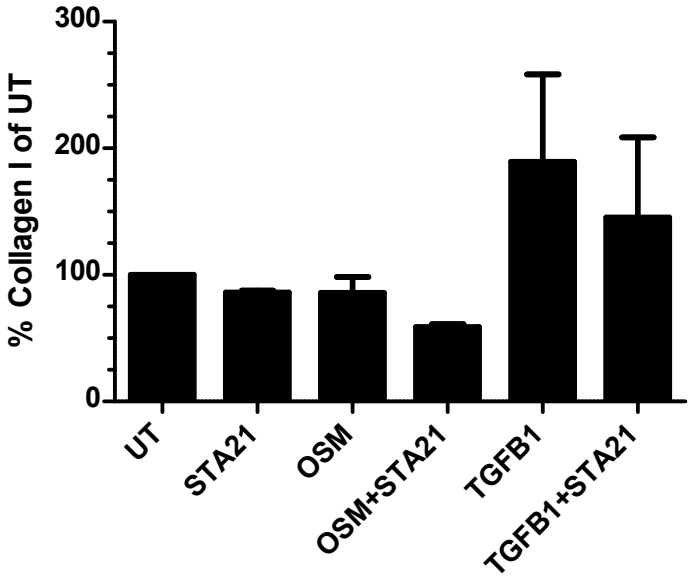

Figure 19. Effect of OSM and STA-21 on collagen-1 protein expression and secretion in primary normal bronchial fibroblasts. Fibroblasts were treated with STA-21 (10 uM) only, OSM (2 ng/ml) only, STA-21 and OSM, TGFβ1 (1 ng/ml) only, TGFβ1 and STA-21 or left untreated. TGFβ1 represents a positive control. STA-21 treatment was one hr prior to OSM or TGFβ1 stimulation for an additional 48 hrs. Secreted protein was measured by western blot analysis and quantified by densitometry. Collagen-1 in the untreated condition is set as 100%, and data is normalized to this value. No statistical significance with one way ANOVA and Bonferroni post-hoc, $p>0.05$, N=3.

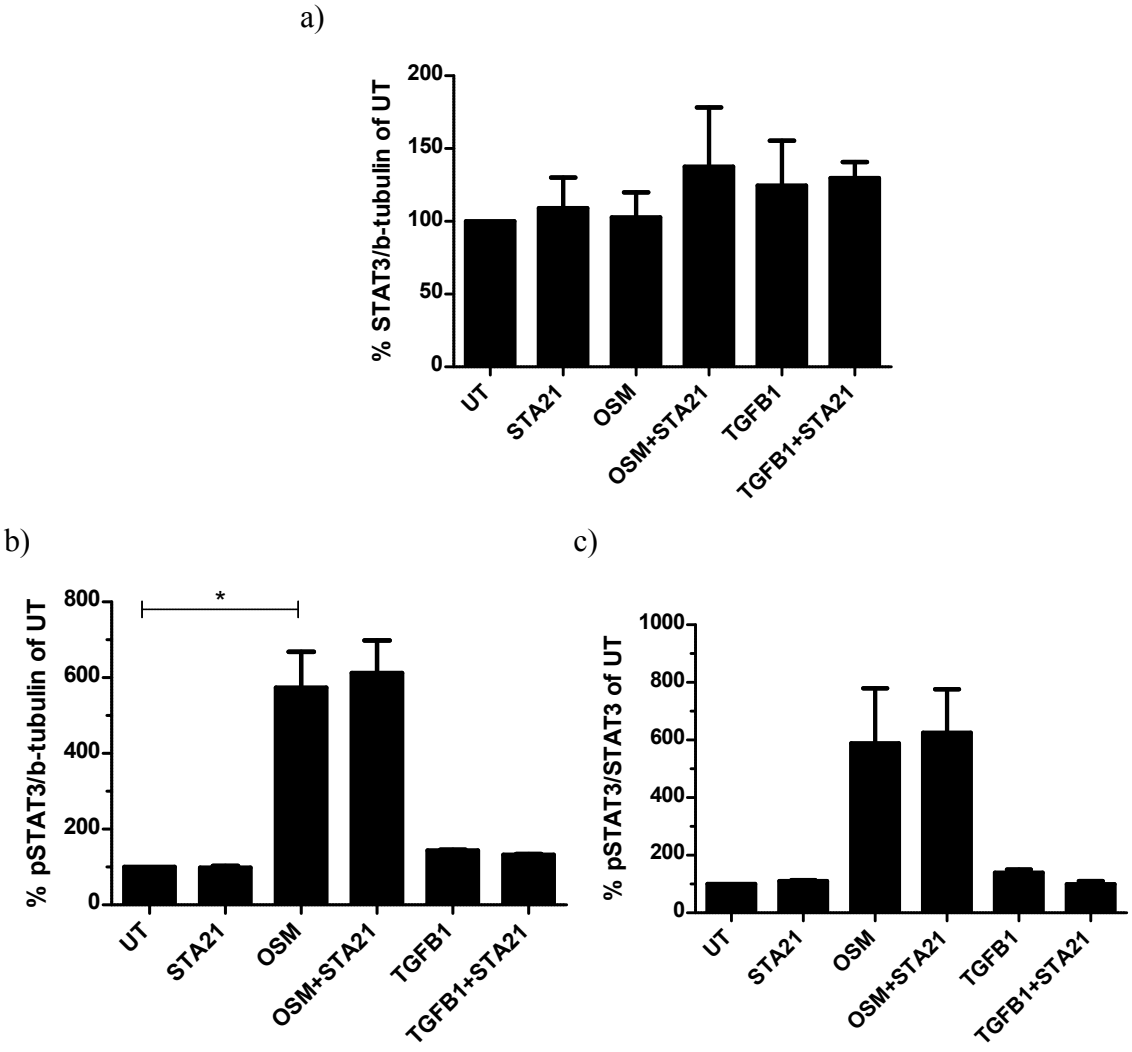

Figure 20. Effect of OSM and STA-21 on EDA-FN protein expression in normal primary bronchial fibroblasts. Fibroblasts were treated with STA-21 (10 uM) only, OSM (2 ng/ml) only, STA-21 and OSM, TGFβ1 (1 ng/ml) only, TGFβ1 and STA-21 or left untreated. TGFβ1 represents a profibrotic positive control. STA-21 treatment was one hr prior to OSM or TGFβ1 stimulation for an additional 48 hrs as an optimal treatment time in HFL fibroblasts. The western blot analysis (a) was quantified by densitometry with β-tubulin as a loading control. EDA-FN expression in the untreated condition is set as 100%, and data is normalized to this value. Statistically significant with one way ANOVA with Bonferroni post-hoc, $p<0.05$, N=3.

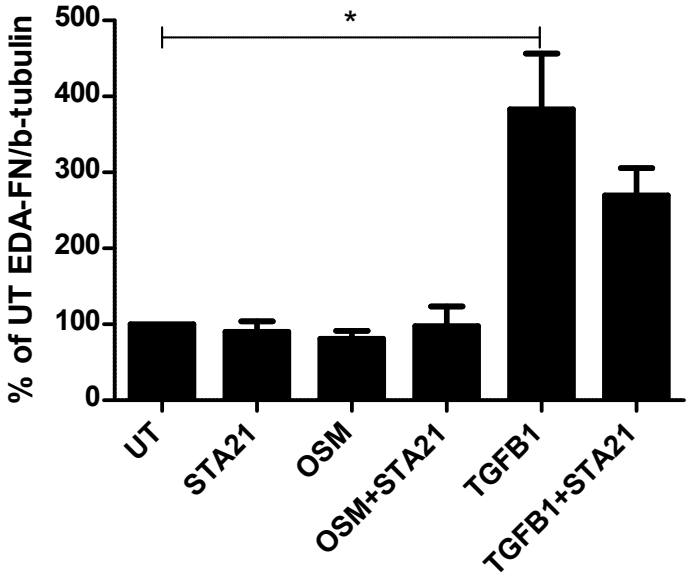

Figure 21. Effect of OSM and STA-21 on EDA-FN protein expression in asthmatic primary bronchial fibroblasts. Fibroblasts were treated with STA-21 (10 uM) only, OSM (2 ng/ml) only, STA-21 and OSM, TGFβ1 (1 ng/ml) only, TGFβ1 and STA-21 or left untreated. TGFβ1 represents a positive control. STA-21 treatment was one hr prior to OSM or TGFβ1 stimulation for an additional 48 hrs. The western blot analysis (a) was quantified by densitometry with β-tubulin as a loading control. EDA-FN expression in the untreated condition is set as 100%, and data is normalized to this value. Statistically significant with one way ANOVA with Bonferroni post-hoc, $p<0.05$, N=3.

3.8. The effect of STAT3 siRNA in primary fibroblasts

In order to determine whether the responses of primary cells to STA-21 were specific, we again turned our attention to STAT3 siRNA. Using this approach, STAT3 expression was significantly knocked-down to a maximum of 75% of the untreated control after 48 hrs in primary normal bronchial fibroblasts (Figure 22a). The transfection reagent and scrambled control had no effect on STAT3 expression. OSM (2 ng/ml) had only a moderate effect with increasing STAT3 expression (in contrast to HFL fibroblasts) approximately 10% more than the untreated control and TGFβ1 had no effect.

As was seen in HFL fibroblasts, STAT3 siRNA decreased STAT3 and total pSTAT3 in primary fibroblasts (Figure 22b) and fractional pSTAT3 increased nearly 50% (Figure 22c), which corresponded with an increase in EDA-FN expression (Figure 22d). Exposure to OSM (2 ng/ml) significantly increased total and fractional pSTAT3 more than 300% and increased EDA-FN expression by approximately 50%. As with STA-21 in primary fibroblasts, STAT3 siRNA significantly inhibited OSM induced total pSTAT3 to the untreated level, but interestingly, STAT3 siRNA significantly helped to increase OSM induced increase in fractional pSTAT3, whereas with STA-21, fractional pSTAT3 remained similar to OSM treatment alone. Also similar to HFL fibroblasts, double stimulation with OSM had no effect on STAT3 expression in primary fibroblasts, but it sustained the increase in total and fractional pSTAT3. Yet different from HFL fibroblasts (no increase in EDA-FN), the increase in EDA-FN was sustained at nearly 100% more than the untreated control. And also different from HFL fibroblasts, STAT3 siRNA did not inhibit OSM induced EDA-FN expression.

TGFβ1 (1 ng/ml) had no effect on STAT3 expression and activity, but EDA-FN expression was increased by approximately 150% of the untreated control. STAT3 siRNA did not inhibit TGFβ1 induced EDA-FN.

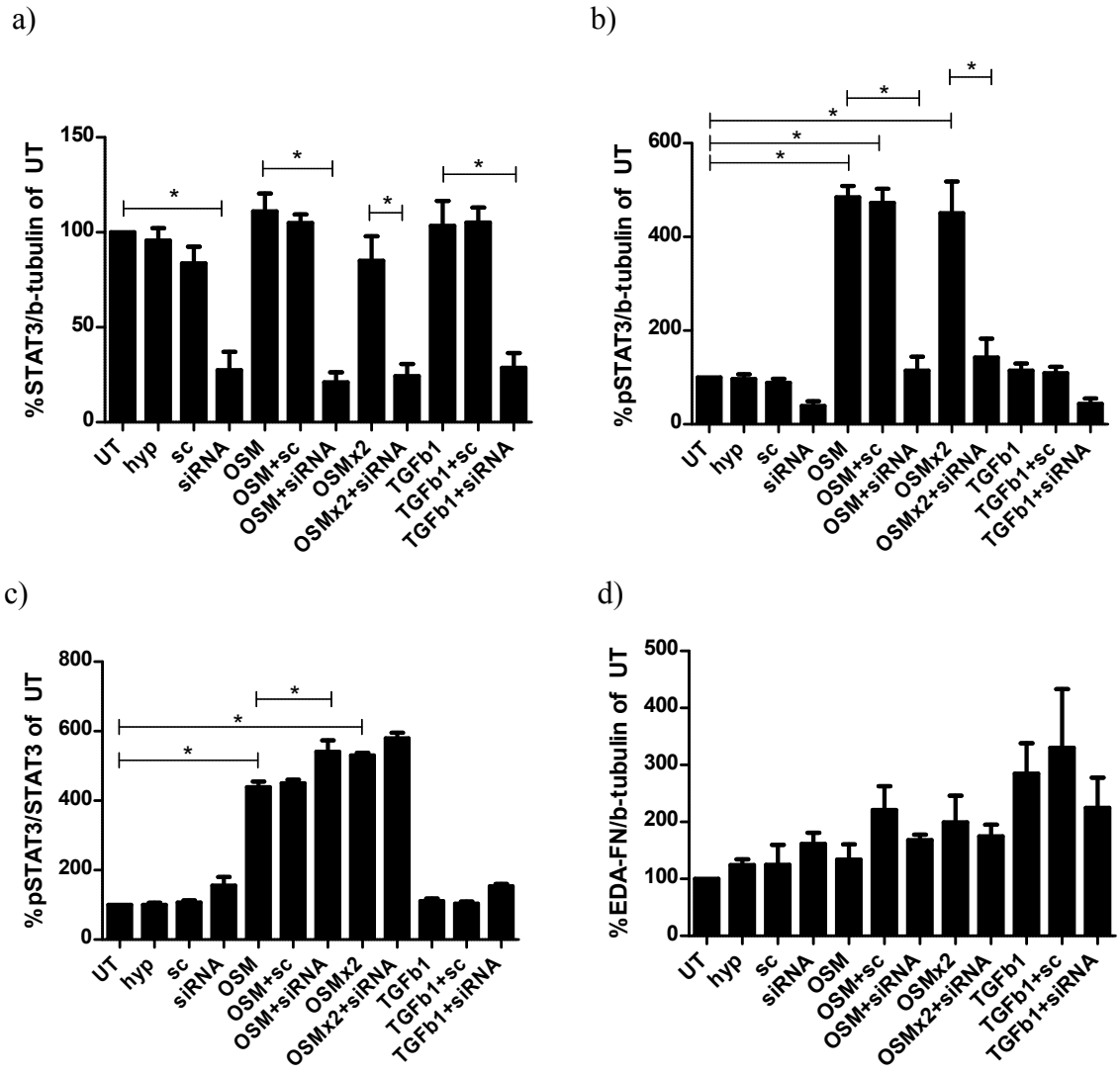

Figure 22. Effect of STAT3 knock-down on STAT3 activity and EDA-FN protein expression with OSM stimulation in normal primary fibroblasts. A pool of four STAT3 siRNAs (25 nM) was added for 48 hrs, followed by OSM (2 ng/ml) or TGFβ1 (1 ng/ml) for an additional 48 hrs. OSM was either re-added or not after the first 24 hrs. OSM increased STAT3 activity and EDA-FN, but there was little increase in STAT3 expression, and STAT3 knockdown by siRNA significantly inhibited OSM induced total and fractional pSTAT3, but did not inhibit OSM induced EDA-FN. Re-addition of OSM increased total and fractional pSTAT3 and EDA-FN. Statistical significance with one way ANOVA and Bonferroni post-hoc test, $p<0.05$, N=3.

3.9. The effect of STAT3 on proliferation of HFL fibroblasts

Increased cell proliferation is another factor that results in ECM protein accumulation and contributes to fibrosis. In attempt to evaluate the effectiveness of modulating STAT3 in fibrotic conditions, STA-21 was used. OSM (2 ng/ml) stimulation for 48 hrs increased proliferation of HFL fibroblasts approximately 50% compared to the unstimulated control (Figure 23). Treatment with STA-21 (10 uM) had no effect on proliferation *per se*, but it inhibited OSM induced proliferation to levels comparable to the untreated control. The positive control 10% FBS induced proliferation more than 100% of the untreated control.

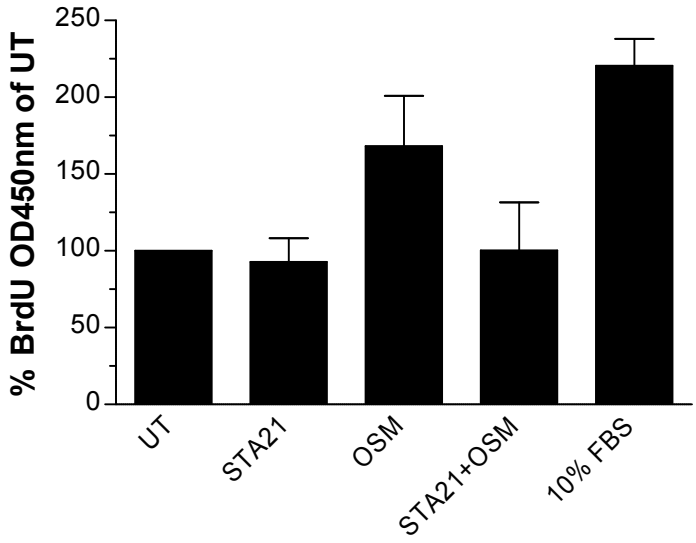

Figure 23. Effect of STA-21 on OSM induced proliferation in HFL fibroblasts. STA-21 (10 uM) was pretreated 1 hr prior to stimulation with OSM (2 ng/ml). Fixed fibroblasts were immunostained with BrdU, and the rate of BrdU incorporation was quantified by hydrogen peroxidase activity. The untreated and unstimulated condition represents the untreated control (UT), where proliferation was set as 100%. All proliferation rates were normalized to the UT control. 10% FBS represents the positive control.

3.10. The effect of STAT3 on proliferation of primary fibroblasts

In contrast to HFL fibroblasts, OSM (2 ng/ml) stimulation decreased proliferation of primary bronchial fibroblasts to approximately 75% of that in the untreated control (Figure 24). Proliferation after treatment with STA-21 was similar to that of the untreated control, but it inhibited OSM repressed proliferation that was comparable to the untreated control. As shown previously, TGFβ1 (1 ng/ml) did not influence proliferation. Pre-treatment with STA-21 had no effect on TGF β1 in proliferation.

a)

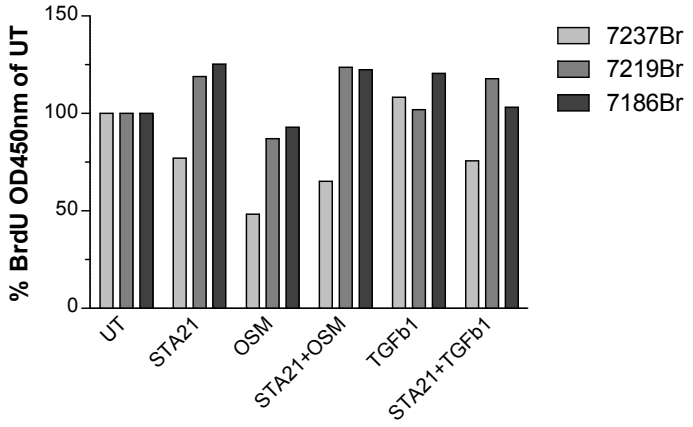

b)

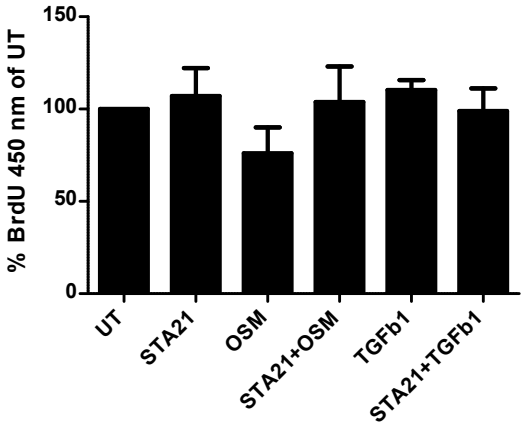

Figure 24. Effect of STA-21 on OSM induced proliferation in primary bronchial fibroblasts. STA-21 (10 uM) was pretreated 1 hr prior to stimulation with OSM (2 ng/ml) or TGFβ1 (1 ng/ml). Fixed fibroblasts were immunostained with BrdU, and the rate of BrdU incorporation was quantified by hydrogen peroxidase activity. The untreated condition represents the untreated control (UT), where proliferation was set as 100%. All proliferation rates were normalized to the UT control. Data presented for each lung fibroblast donor (a) or as an average (b). N=3.

3.11. The relative roles of STAT3 and ERK in HFL proliferation

In order to decipher the differential effects of OSM on cell proliferation in HFL and primary fibroblasts, the two downstream signaling pathway of OSM were inhibited one at a time. STAT3 inhibitor STA-21 (10 uM) and ERK1/2 inhibitor UO126 (10 uM) alone produced negligible effects on proliferation in HFL fibroblasts (Figure 25). OSM (2 ng/ml) stimulation increased proliferation by 50% compared to the untreated control. Both STA-21 and UO126 inhibited OSM induced proliferation to control levels, and they provided controversial additive effect when used in combination. Positive control 10% FBS increased proliferation by 100% of the untreated control.

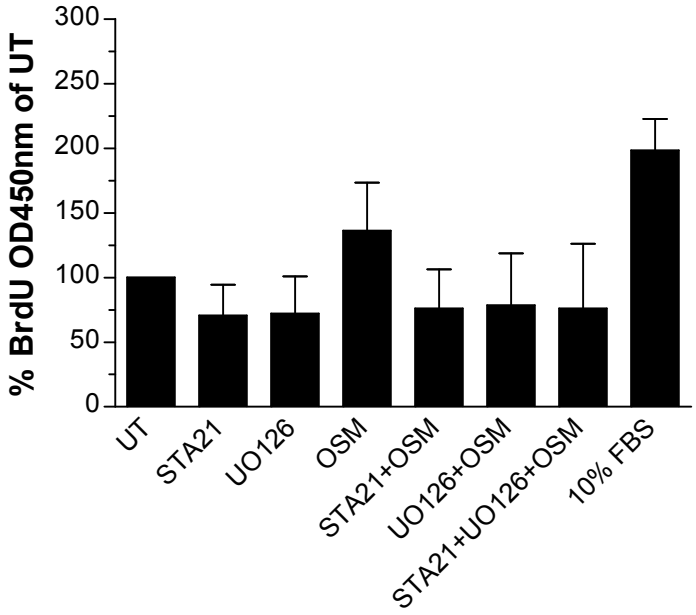

Figure 25. Effect of STA-21 and UO126 on OSM induced proliferation in HFL fibroblasts. STA-21 (10 uM) and UO126 (10 uM) had no effect on proliferation. OSM (2 ng/ml) stimulation for 48 hrs increased proliferation, and 1 hr pretreatment with STA-21 or UO126 alone or in combination inhibited OSM induced proliferation to the untreated (UT) rate. 10% FBS represents the positive control. No statistical significance with one way ANOVA and Bonferroni post-hoc, $p<0.05$, N=2.

Chapter 4. Discussion

4.1. Summary of main findings

In this thesis, we showed that expression of the pro-fibrotic ECM protein EDA-FN is induced by STAT3 activation following exposure to OSM in HFL fibroblasts. We showed dependency on STAT3 activity by both inhibition of STAT3 nuclear translocation using a small molecule inhibitor and STAT3 protein expression with RNA interference. In contrast, exposure to a variety of cytokines that activate STAT3 through gp130 had no effect on expression of collagen-1. This pathway also appeared to mediate HFL fibroblast proliferation. Unexpectedly, STAT3 signalling was not involved in the induction of EDA-FN expression and even appeared to inhibit proliferation in primary adult fibroblasts. The reasons underlying the disparate effects of STAT3 activation on EDA-FN expression and proliferation in fetal and adult fibroblasts remain to be elucidated.

The experiments described in this thesis were designed to evaluate the effect of STAT3 activation on indices of fibroblast function that relate to fibrosis. Initial experiments were conducted to define the rank order of potency and optimal time of exposure to the STAT3-activating IL-6 cytokine. Stimulation with IL-6, LIF or OSM at various concentrations and over a time course induced transient and phasic increases in cellular EDA-FN, but not secreted collagen-1. The order of cytokine potency was: OSM = LIF > IL-6. The reason for this is unknown, but is possibly due to expression of their different receptor subunits. The IL-6 receptor complex exists as a dimer of transmembrane gp130 subunits with an additional IL-6α receptor, while OSM receptor complex exists as a dimer of gp130 and OSM receptor subunits

(including OSMRβ) and LIF receptor complex exists as a dimer of gp130 and LIF receptor subunits (including LIFRα/β) (Heinrich *et al.* 2003). The expression of IL-6Rα is tightly regulated with increased cell surface expression upon stimulation, and thus, higher concentrations of IL-6 are needed to produce similar increases in EDA-FN compared to OSM and LIF. Expression of LIFRα/β and OSMRβ expression is also regulated, albeit to a lesser extent (Heinrich *et al.* 1998). The greater potency of OSM could be also explained by the presence of a rarely conserved amino acid motif Box 3 in the intracellular domain of the receptor that is necessary for the action of OSMR, although it is unnecessary for LIFR and gp130 (Kuropatwinski *et al.* 1997). Furthermore, the number and position of tyrosine residues available for phosphorylation in the cytoplasmic portion of the three receptor subunits vary. OSMR and LIFR share three homologous tyrosine residues, but none of these are found in gp130. The difference in effect due to OSM and LIF is mainly a result of the unique type II OSMR (OSMRβ). Nevertheless, since activation of IL-6, OSM and LIF receptors increases downstream STAT3 activity and EDA-FN expression, our data supports the hypothesis of a correlation between STAT3 activity and EDA-FN protein expression.

The increase in basal EDA-FN expression over time in the untreated controls represents accumulative protein expression is most likely due to increased cell number. The doubling time of HFL fibroblasts is approximately 24 hrs (laboratory observation), with EDA-FN expression at 48 hrs is approximately doubled compared to at 24 hrs. In addition, increased cell number allows for increased cell surface β1 integrin interaction with EDA-FN, and it has been shown that β1 integrin adhesion enhances IL-6 mediated STAT3 signaling (Shain *et al*. 2009).

The phasic increases in EDA-FN over the course of 72 hrs is possibly due to STAT3 feedback inhibition of signaling by suppressor of cytokine signaling (SOCS)-3. SOCS3 is a transcriptional target of STAT3 and acts as a negative regulator by interacting with the receptor associated JAK to prevent phosphorylation of STAT3. It also targets STAT3 to the proteasome for ubiquitination. SOCS3 is rapidly induced but has a short half-life (approximately 1.5 hrs (Auernhammer & Melmed 2001). Expression of individual receptor subunits (chains) and their recruitment to the cell surface is also involved in negative feedback. OSM first decreases gp130 and OSMRβ protein by ligand-induced degradation and thereafter increases their cell surface expression by enhanced synthesis (Blanchard *et al.* 2001).

It has been previously shown that STAT3 contributes to keloid pathogenesis via promoting collagen production (Lim *et al.* 2006). However, the lack of observed effect of IL-6 cytokines on collagen-1 expression in HFL fibroblast can be explained by several possible mechanisms. First, there may be differences in response in fetal and adult fibroblasts. For example, embryonic skin fibroblasts are less prone to cell differentiation into myofibroblasts, have high levels of hyaluronic acid and produce scar-free wound healing (McCallion & Ferguson 1997). On the other hand, adult skin fibroblasts can more easily differentiate into myofibroblasts leading to excessive accumulation of ECM proteins, including collagen, and wound healing results in a scar (Ferguson & O'Kane 2004). Alternatively, HFL fibroblasts may express higher levels of fibroblast growth factor (FGF), which are mitogens that allow rapid cell growth (Vlodavsky *et al.* 1990). FGFs bind to heparin, which is an anti-coagulant that inhibits collagen crosslinking and enhances collagen degradation. Potentially increased FGFs in HFL fibroblasts may be associated with an increase in heparin levels and decreased collagen accumulation. It has been

shown that heparin inhibits epidermal growth factor, which leads to decreased inflammatory cell number and scarring (Imaizumi *et al.* 1996). Secondly, collagen-1 can be degraded by matrix metalloproteinase (MMP)-1. It has been shown that STAT3 activation up-regulates the expression of MMP-1 in kidney fibroblasts (O'Kane *et al.* 2009). In addition, the MMP-1 gene promoter contains an OSM-responsive element (OMRE) that encompasses the STAT binding element (Korzus *et al.* 1997). Thus, collagen-1 may be expressed and secreted, but is cleaved by STAT3-induced MMP-1. One way to address this would be to measure whether collagen gene expression is modulated by OSM. Thirdly, fibronectin is the prototype cell adhesion protein that adheres fibroblasts to the ECM. As cell-matrix communication is an important determinant for cell growth and differentiation, in an *in vitro* system, fibronectin, and not collagen, plays the primary role in fibroblast growth and differentiation (Bitterman *et al.* 2011). However, in an *in vivo* system, a multicellular microenvironment and epithelial-mesenchymal transition contribute to increased collagen secretion as the fibroblast population grows (Westerngren-Thorsson *et al.* 1993).

Upon recruitment and activation STAT3 translocates into the nucleus where it initiates gene transcription. A small molecule inhibitor STA-21 was used to block this process. STA-21 is proposed to form hydrogen bonds with three amino acid residues in the SH2 domain of STAT3 (R595, R609 and I634) so that STAT3 molecules are prevented to interact with each other and dimerize via their SH2 domains, which is a pre-requisite for nuclear translocation to transcribe its target genes (Song *et al*. 2005). We showed that STA-21 inhibits nuclear translocation of pSTAT3 by immunofluorescence, and this supports the proposed mechanism of action by STA-21 (Song *et al.* 2005). To date, the inhibitory effect of STA-21 has only been assessed by decreasing STAT-3 dependent luciferase activity. Herein, we provide the first imaging evidence

that it prevents nuclear translocation of STAT3. There is little or no pSTAT3 in the absence of OSM stimulation, but its expression is up-regulated in the presence of OSM. Pretreatment with STA-21 substantially inhibits nuclear pSTAT3 instead causing peri-nuclear aggregation.

STAT3 activity is transient under normal conditions. Our data support this as there was no significant increase in pSTAT3 after a single OSM stimulation after 48 hrs in HFL fibroblasts. In contrast, repeated exposure to OSM, which might occur in pathological situations, substantially sustained STAT3 activation. The increased pSTAT3 was a result of increased STAT3 expression, which increases the STAT3 pool available to become phosphorylated. Thus, both total and fractional pSTAT3 were increased. Along the same lines, repetitive dosing of STA-21 produced significant inhibition of OSM induced STAT3 activity

Having established baseline conditions, we next sought to examine the effect of STAT3 on EDA-FN expression. Basal expression of EDA-FN protein in the absence of exogenously applied OSM is possibly due to growth factor and cytokine-rich FBS or autocrine/paracrine of growth factor or cytokine secretion. The constitutive expression of low levels of EDA-FN was complemented by minimal, but observable pSTAT3, suggesting that pSTAT3 may have contributed to basal EDA-FN expression, but this does not rule-out other potential STAT3 independent mechanisms. Fibronectin is required for embryonic development, and inactivating the gene for fibronectin leads to early embryonic lethality (George *et al.* 2003). As such, basal fibronectin expression is not unexpected. The robust increase in pSTAT3 after OSM reinforces that STAT3 has inducible transient activity under normal conditions, but is sustained by re-addition every 24 hrs to mimic pathological conditions. Using this strategy we show that OSM

added every 24 hrs induced EDA-FN expression suggesting that EDA-FN is a downstream effector of OSM. This is supported by the observation that STA-21 could potently inhibit OSM induced EDA-FN expression. Disruption of the STAT3 gene is also embryonically lethal (Takeda *et al.* 1997). The requirement of both fibronectin and STAT3 genes for embryonic development suggests a potential link between STAT3 signaling and fibronectin expression. Fibroblasts have many homeostatic mechanisms to maintain a relatively constant level of STAT3 expression. That the relative expression of pSTAT3 following OSM exposure was maintained in the presence or absence of STA-21 supports the proposed mechanism of action of STA-21 in that it does not prevent pSTAT3 phosphorylation, but only pSTAT3 nuclear translocation (Song *et al.* 2005). The decreased total pSTAT3 and STAT3 protein suggests a second potential mechanism of action of STA-21: it decreases STAT3 protein expression, which decreases the STAT3 pool available for phosphorylation.

4.2. STAT3 siRNA with OSM stimulation in HFL fibroblasts

Given that small molecule inhibition may be associated with off-target effects we also examined the effects of siRNA to STAT3. We showed that using a pool of four siRNAs was extremely effective at knocking down STAT3 expression. This approach also potently suppressed OSM induced EDA-FN corroborating the data seen when using STA-21. These data strongly suggest that EDA-FN expression is dependent upon STAT3 activation.

The prototype effector transcription factor in the fibrotic response of TGFβ1 is Smad3, and the conventional STAT3 activation pathway by IL-6 family cytokines crosstalks with the TGFβ1 signaling pathway via Smad7 (Ono *et al.* 2008, Jenkins *et al*. 2005). STAT3 induces Smad7 expression, which acts as a negative regulator of TGFβ and inhibits Smad3 phorphorylation and downstream transcription of its target genes (Merchant 2008, Yan *et al.* 2009). Yet the exact mechanism of crosstalk remains to be elucidated. TGFβ1 also activates various downstream cellular signaling pathways that lead to STAT3 activation. For example, TGFβ induces fibronectin synthesis through transcription factor c-Jun, which has a DNA binding site close to that of STAT3 (Zhang *et al.* 1999). Their DNA binding sites are independent, but cooperative interaction between c-Jun and STAT3 may serve as function enhancers. Also, PI3K/Akt modulates STAT3 mediated gene expression (Kortylewski *et al.* 2002). In addition, p38 and JNK regulate STAT3 activity by serine phosphorylation (Turkson *et al*. 1999). In this study, STAT3 knockdown had little effect on the ability of TGFβ1 to induce EDA-FN, suggesting that TGFβ1 induced EDA-FN expression is not dependent on STAT3 activation. In this context,

TGFβ1 has been shown to promote STAT3-dependent fibronectin expression in human proximal tubular epithelial cells (Giannopoulou *et al.* 2006).

4.3. STAT3 inhibition by STA-21 in primary adult fibroblasts

The purpose of these experiments was to compare responses of fetal lung fibroblast to primary cultures of adult fibroblasts. The rationale is that fetal fibroblasts do not repair with scarring, whereas adult cells do (McCallion & Ferguson 1997). With scarring in adult fibroblasts, they have a greater potential to produce more ECM proteins, and individuals with IPF are adults usually greater than 50 years of age.

The magnitude of EDA-FN expression after exposure to OSM in fetal and primary adult fibroblasts was dissimilar. The reasons behind disparate effects of IL-6 cytokines in fetal and adult cells remain unknown, although they may be related to the age of donors and their state of cellular differentiation and altered signaling. For example, normal growing fetal fibroblasts progress through the cell cycle faster than the differentiating adult fibroblasts (into myofibroblasts) which arrests at the synthesis stage of the cell cycle for a longer duration to produce proteins. In other words, fetal fibroblasts can simultaneously proliferate and express ECM proteins, leading to their rapid accumulation, while adult fibroblasts cannot express proteins during proliferation (McCallion & Ferguson 1997). Furthermore, increased degradation of existing collagen-1 is associated with increased secretion of metalloproteinase-1 (MMP1), by fetal fibroblasts (McCallion & Ferguson 1997, Schwartzkopff *et al.* 2002). Consequently, increased degradation of soluble ECM proteins allows fibroblasts to enhance their production and secretion of insoluble cellular EDA-FN to replace the degraded ECM (Valenick *et al.* 2005).

The association of OSM induced increased pSTAT3 with decreased EDA-FN and collagen-1 expression in adult primary fibroblasts may be attributed to cell adaptation to withstand minor pro-inflammatory stimuli and to protect themselves from injury, that is, they are more resistant to damage. For example, the threshold for pSTAT3 induced EDA-FN and collagen may be higher in adult fibroblasts than that in fetal fibroblasts. However, EDA-FN response to TGFβ1 is maintained and is not inhibited by a STAT3 inhibitor. This suggests potential STAT3-independent signaling pathway after TGFβ1 stimulation.

Another possible explanation is that the wound healing process is slower in adult fibroblasts compared to fetal fibroblasts. Perhaps fetal fibroblasts can degrade existing ECM proteins and replace with new ECM proteins within 48 hrs of OSM stimulation, while adult fibroblasts have only degraded existing ECM proteins and are in the process of replacement/expression of new ECM proteins during the same time period. Fibroblasts display heterogeneity in that fibroblasts isolated from different parts of the lung may respond differently to the same cytokines. More specifically, lung parenchyma, but not proximal bronchi, produces fibroblasts with enhanced TGFβ signaling and α-SMA expression (Peckovsky *et al*. 2010). We used adult bronchial fibroblasts in this study, since these cells express higher basal levels of pSTAT3.

Previous work from our laboratory, has previously shown that primary fibroblasts isolated from normal healthy individuals and patients with IPF differ in IL-6 signaling (Moodley *et al.* 2003). More specifically, IL-6 is a mitogen in IPF fibroblasts that is MAPK dependent, but IL-6 decreases proliferation in normal fibroblasts which is STAT3 dependent. In addition, IL-6 is

anti-apoptotic in IPF fibroblasts, but IL-6 is pro-apoptotic in normal fibroblasts. Since IL-6 and OSM activate a common gp130 receptor subunit, we expected similar effects.

The reversal of OSM induced repression of EDA-FN expression by STA-21 in primary normal fibroblasts suggests that the effect is STAT3 dependent, but why EDA-FN is decreased in adult cells is unknown. We have attempted to address the disparate effects by testing the hypothesis of divergent OSM downstream signaling, which is explained below.

Indifferent effects of OSM and STAT3 inhibition in adult primary normal and asthmatic fibroblasts suggests that STAT3 signaling is similar in normal and asthmatic conditions. Yet, the larger increase in EDA-FN expression after TGFβ1 in asthmatic fibroblasts is not surprising as asthma is associated with increased secretion of and response to pro-inflammatory cytokines. The differences may also be a result of lung heterogeneity, or the disparate locations that the fibroblasts were isolated.

4.4. Effect of STAT3 knock-down on EDA-FN expression in primary adult fibroblasts

The purpose of using siRNA is to confirm the results obtained using STA-21. Knock-down of STAT3 by siRNA does not totally deplete STAT3 expression and as such, STAT3 phosphorylation remains possible. Thus, total and fractional pSTAT3 after OSM stimulation in the presence of STAT3 knockdown are still greater than the untreated control.

Reversal of EDA-FN expression after single treatments of OSM with STAT3 knockdown corroborates with STAT3 inhibition by STA-21 in primary normal fibroblasts. This confirms that changes EDA-FN expression is dependent upon STAT3 activity. However, the STAT3 and ERK pathways need to be examined in more detail to conclude whether the relationship between EDA-FN expression and STAT3 activity is positively or negatively correlated. As was seen for HFL, we saw no effect of STAT3 knockdown on TGFβ1 induced EDA-FN in primary normal fibroblasts.

4.5. Effect of STA-21 on proliferation of HFL and primary adult fibroblasts

Previous work from our laboratory has shown that OSM is a mitogen in HFL fibroblasts and it is mediated by STAT3 signalling (Scaffidi *et al.* 2002). However, OSM decreased proliferation in primary normal fibroblasts, despite this is also mediated by STAT3 signaling. Previously published data suggests that OSM modulates cell proliferation either positively or negatively depending on the target cell (Tanaka & Miyajima 2003). For example, human OSM stimulates the growth of AIDS-related Kaposi's sarcoma cells (Miles *et al.* 1992) and plasmacytoma cells (Nishimoto *et al.* 1994), but it inhibits the growth of lung cancer cells (Horn *et al.* 1990) and normal breast epithelial cells (Grant *et al.* 2001). Similar results have been shown using murine OSM. Thus, OSM induces differentiation in fetal hepatocytes and down-regulates cell cycle progression cyclin D expression via STAT3, while it induces expression of cyclin D in adult hepatocytes (Matsui *et al*. 2002). The published data showing a differential effect of OSM on proliferation in fetal and adult hepatocytes supports our observations in fetal and adult lung fibroblasts. In particular, it proposes that proliferation and function are inversely related so that

fetal cells proliferate faster, but lack most mature liver cell functions in the adult and vice versa. Application of OSM will induce the opposite effect.

As previously mentioned, primary fibroblasts isolated from normal healthy individuals and patients with IPF differ in IL-6 signaling in terms of proliferation and apoptosis. IL-6 is a mitogen in IPF fibroblasts, but it decreases proliferation in normal fibroblasts. In IPF fibroblasts, there is decreased cell cycle inhibitor p27Kip1 and increased expression of cyclin D1 and therefore, more cells are engaged in cell cycle progression. In normal fibroblasts, there is increased inhibitor of cell cycle progression p19NK4D (Moodley *et al*. 2003) In terms of apoptosis, IL-6 is anti-apoptotic in IPF fibroblasts, with increased expression of anti-apoptotic protein Bcl-2, but IL-6 is pro-apoptotic in normal fibroblasts with increased expression of pro-apoptotic protein Bax (Moodley & Misso *et al.* 2003). However, IL-11 is a mitogen and decreases apoptosis in both IPF and normal fibroblasts. Furthermore, our lab has shown that OSM is a positive modulator of proliferative activity in both HFL and IPF (unpublished observation). In addition, the enhancement on proliferation and inhibition on apoptosis in HFL fibroblasts suggests that OSM has pro-fibrotic properties (Scaffidi *et al.* 2002). This also suggests that OSM may play a role in lung wound repair and fibrosis in IPF fibroblasts. As mentioned earlier, normal adult lung fibroblasts may have adapted mechanisms such that a minor insult is not pathological. In fact, OSM displays unique effects in adult and fetal fibroblasts accordingly. OSM can modify EDA-FN and ECM proteins. OSM potentially decreases EDA-FN protein expression and decreases cell proliferation in normal adult fibroblasts, which is anti-fibrotic, while OSM increases EDA-FN protein expression and increases cell proliferation in fetal fibroblasts (and potentially IPF fibroblasts), which is pro-fibrotic. Despite whether OSM is

anti- or pro-fibrotic, its effects are mediated by STAT3, as STAT3 inhibition by STA-21 reverses OSM activity in both adult and fetal lung fibroblasts. This suggests that inhibiting STAT3 activity may be a potential therapeutic target for treatment of patients with IPF.

Our data shows that TGFβ1 is not a mitogen in primary normal bronchial fibroblasts. It was previously showed that TGFβ induced human lung fibroblast proliferation at low doses while it inhibited proliferation at high doses, yet both were due to an increase in cyclooxygenase-mediated PGE2 production (McAnulty 1997).

4.6. Effect of inhibiting STAT3 or ERK 1/2 on proliferation of HFL fibroblasts

To evaluate the divergent downstream signalling of OSM, STAT3 and ERK1/2 were inhibited either alone or in combination in HFL fibroblasts. Incubation with STA-21 or UO126 in the absence of any other stimulation did not modify proliferation of HFL fibroblasts. Somewhat surprisingly, OSM-induced proliferation was dependent upon both STAT3 and ERK1/2 activation since inhibition of either reduced proliferation. This is an important finding as altered signalling that favours either pathway is potentially pathological. For example, in cancerous cells, STAT3 signalling is favoured over ERK1/2. In adult normal fibroblasts, increases in STAT3 decreases proliferation while in adult IPF fibroblasts, increases in ERK increases proliferation (Moodley *et al.* 2003).

Despite similarities between the STAT3 and ERK1/2 signalling pathways, there are noticeable differences in their mode of activation. STAT3 is activated by phosphorylation of up to four tyrosine residues on gp130 and one residue on the OSMR subunit, while ERK is activated

following phosphorylation of only one tyrosine residue on gp130. Thus, the OSMR complex is potentially a more potent activator of STAT3 compared to ERK1/2. Also, activation of STAT3 by OSM induces gp130 expression, leading to a further increase in activation of STAT3, while activation of ERK promotes OSMRα degradation, leading to a decrease in STAT3 activation with a proportionate increase in ERK activity and a further increase in ERK recruitment and activation (Blanchard *et al.* 2001). As mentioned previously, proliferation due to STAT3 or ERK is cell type dependent. Based on our own observations, HFL fibroblasts resemble those isolated from IPF patients, thus by inhibiting STAT3, OSM signalling favours the ERK pathway, which induces OSMRα degradation to increase ERK activity and proliferation in HFL fibroblasts. By inhibiting ERK, OSM signalling favours the STAT3 pathway, which induces gp130 surface expression to increase STAT3 activity and increase or decrease proliferation (depending on the cell type).

Chapter 5. Conclusion

The data presented in this thesis shows that expression of the pro-fibrotic ECM protein EDA-FN and increased cellular proliferation of fetal lung fibroblasts are dependent upon STAT3 activation. This dependency on STAT3 activity was confirmed by both small molecule inhibition and RNA interference. As a result, inhibition of STAT3 activity may be a potential pharmacological target for treatment of patients with pulmonary fibrosis. However, in primary cultures of adult fibroblasts, which more closely resemble the realistic pulmonary fibrotic condition in adult patients, OSM had no effect on EDA-FN expression and decreased cellular proliferation, but exposure to TGFβ1 induced EDA-FN in both cell types that were not STAT3-dependent. Alteration of the STAT3 and ERK1/2 pathways in attempt to explain the differential effects of OSM in fetal and adult fibroblasts revealed that they display similar effects and suggested that pathological adult fibroblasts need to be examined.

Chapter 6. Future Studies

EDA-FN expression and cell proliferation can be evaluated in fibroblasts obtained from IPF patients to compare with normal healthy individuals. The divergent STAT3 and ERK1/2 signalling can be examined in IPF fibroblasts using their respective inhibitors, STA-21 and UO126, to compare with normal healthy individuals and/or HFL fibroblasts. Other end-point measurements of STAT3 inhibition in fibroblasts could include cell apoptosis and migration. An animal model of pulmonary fibrosis could be used to evaluate the effect of STAT3 inhibition as a potential treatment.

REFERENCES

Armanios, M., Chen, J., Cogan, J., Aider, J., Ingersoll, R., Markin, C., Lawson, W., Xie, M., Vulto, I., Phillips, J., Lansdorp, P., Greider, C. and Loyd, J. **Telomerase Mutations in Families with Idiopathic Pulmonary Fibrosis.** *The New England Journal of Medicine*, 2007; **356**: 1317-1326.

Auernhammer, C. and Melmed, S. **The central role of SOCS-3 in integrating the neuro-immunoendocrine interface.** *The Journal of Clinical Investigation*, 2001; **108**(12): 1735-1740.

Bitterman, P., Rennard, S., Adelberg, S. and Crystal, R. **Role of Fibronectin in Fibrotic Lung Disease: A Growth Factor for Human Lung Fibroblasts.** *CHEST*, 2011: Supplement 96S.

Blanchard, F., Wang, Y., Kinzie, E., Duplomb, L., Godard, A. and Baumann, H. **Oncostatin M regulates the synthesis and turnover of gp130, leukemia inhibitory factor receptor alpha, and oncostatin M receptor beta by distinct mechanisms.** *Journal of Biological Chemistry*, 2001; **276**(50): 47038-47045.

Chung, J., Uchida, E., Grammer, T. and Blenis, J. **STAT3 Serine Phosphorylation by ERK-Dependent and –Independent Pathways Negatively Modulates Its Tyrosine Phosphorylation.** *Molecular and Cellular Biology*, 1997; **17**(11): 6508-6516.

Elias, J.A., Freundlich, B., Kern, J.A. and Rosenbloom, J. **Cytokine networks in the regulation of inflammation and fibrosis in the lung.** *Chest*, 1990; **97**(6): 1439-1445.

Dauer, D., Ferraro, B., Song, L., Yu, B., Mora, L., Buettner, R., Enkemann, S., Jove, R. and Haura, E. **Stat3 regulates genes common to both wound healing and cancer.** *Oncogene*, 2005; **24**: 3397-3408.

Du Bois, R.M. **Strategies for treating idiopathic pulmonary fibrosis**. *Nature Reviews Drug Discovery*, 2010; **9**: 129-140.

Dugina, V., Fontao, L., Chaponnier, C., Vasiliev, J. and Gabbiani, G. **Focal adhesion features during myofibroblastic differentiation are controlled by intracellular and extracellular factors.** *Journal of Cell Science,* 2001; **114**(18): 3285-3296.

Duncia, J.V., Santella, J.B., Higley, C.A., Pitts, W.J., Wityak, J., Frietze, W.E., Rankin, F.W., Sun, J.H., Earl, R.A., Tabaka, A.C., Teleha, C.A., Blom, K.F., Favata, M.F., Manos, E.J., Daulerio, A.J., Stradley, D.A., Horiuchi, K., Copeland, R.A., Scherle, P.A., Trzaskos, J.M., Magolda, R.L., Trainor, G.L., Wexler, R.R., Hobbs, F.W. and Olson, R.E. **MEK inhibitors: the chemistry and biological activity of UO126, its analogs and cyclization products.** *Bioorganic and Medicinal Chemistry Letters*, 1998; **8**(20): 2839-2844.

Ferguson, M.W.J. and O'Kane, S. **Scar-free healing: from embryonic mechanisms to adult therapeutic intervention.** *The Royal Society*, 2004; **359**: 839-850.

George, E.L., Georges-Labouesse, E.N., Patel-King, R.S., Rayburn, H. and Hynes, R.O. **Defects in mesoderm, neural tube and vascular development in mouse embryos lacking fibronectin.** *Development*, 2003; **119**(4): 1079-1091.

Giannopoulou, M., Iszkula, S., Dai, C., Tan, X., Yang, J., Michalopoulos, G. and Liu, Y. **Distinctive role of Stat3 and Erk-1/2 activation in mediating interferon-γ inhibition of TGF-β1 action.** *American Journal of Physiology – Renal Physiology*, 2007; **290**(5): F1234-F1240.

Grant, S.L., Douglas, A.M., Goss, G.A., Begley, C.G. **Oncostatin M and leukemia inhibitory factor regulate the growth of normal human breast epithelial cells.** *Growth Factors*, 2001; **19**: 153–162.

Heinrich, P., Behrmann, I., Haan, S., Hermanns, H.M., Muller-Newen, G. and Schaper, F. **Principles of interleukin (IL)-6 cytokine signalling and its regulation.** *The Biochemical Journal*, 2003; **374**: 1-20.

Hinz, B, Phaan, S.H., Thannickal, V.J., Galli, A., Bochaton-Piallat, M.L. and Gabbiani, G. **The Myofibroblast, One Function, Multiple Origins.** *The American Journal of Pathology*, 2007; **170**(6): 1-10.

Hosui, A., Kimura, A., Yamaji, D., Zhu, B.M., Na, R. and Hennighausen, L. **Loss of STAT5 causes liver fibrosis and cancer development through increased TGF-β and STAT3 activation.** *The Journal of Experimental Medicine*, 2009; **206**(4): 819-831.

Huang, S. **Regulation of metastases by signal transducer and activator of transcription 3 signalling pathway: clinical implications.** *Clinical Cancer Research*, 2007; 13(5): 1362-1366.

Imaizumi, T., Jean-Louis, F., Dubertret, M. and Dubertret, L. **Herparin induces fibroblast proliferation, cell-matrix interaction and epidermal growth inhibition.** *Experimental Dermatology*, 2006; **5**(2): 89-95.

Jenkins, B.J., Grail, D., Nheu, T., Najdovska, M., Wang, B., Waring, P., Inglese, M., McLoughlin, R.M., Jones, S.A., Topley, N., Baumann, H., Judd, L.M., Giraud, A.S., Boussioutas, A., Zhu, H.J. and Ernst, M. **Hyperactivation of Stat3 in gp130 mutant mice promotes gastric hyperproliferation and desensitizes TGF-beta signaling.** *Nature Medicine*, 2005; **11**(8): 845-852.

Jeon, K.W. International Review of Cell and Molecular Biology, Vol. 276. Burlington: Academic Press, 2009, 161-214.

Jones, K.P., Reynolds, S.P., Capper, S.J., Kalinka, S., Edwards, J.H. and Davies, B.H. **Measurement of interleukin-6 in bronchoalveolar lavage fluid by radioimmunoassay: differences between patients with interstitial lung disease and control subjects.** *Clinical and Experimental Immunology*, 1991; **83**(1): 30-34.

Jordana, M., Richards, C., Irving, L.B. and Gauldie, J. **Spontaneous in vitro release of alveolar-macrophage cytokines after the in tracheal instillation of bleomycin in rats. Characterization and kinetic studies.** *The American Review of Respiratory Disease*, 1988; **137**(5): 1135-1140.

Kato, T., Sakamoto, E., Kutsuna, H., Kimura-Eto, A., Hato, F. and Kitagawa, S. **Proteolytic Conversion of STAT3α to STAT3γ in Human Neutrophiles, Role of Granule-Derived Serine Proteases.** *Journal of Biological Chemistry*, 2004; **279**: 31073-31080.

Keerthisingam, C.B., Jenkins, R.G., Harrison, N.K., Hernandez-Rodriguez, N.A., Booth H., Laurent, G.J., Hart, S.L., Foster, M.L. and McAnulty, R.J. **Cyclooxygenase-2 deficiency results in a loss of the anti-proliferative response to transforming growth factor-beta in human fibrotic lung fibroblasts and promotes bleomycin-induced pulmonary fibrosis in mice.** *American Journal of Pathology*, 2001; **158**: 1411-1422.

Khalil, N. and O'Connor, R. **Idiopathic pulmonary fibrosis: current understanding of the pathogenesis and the status of treatment.** *Canadian Medical Association Journal*, 2004; **171**: 153-160.

Kim, Y.S., Lew, D.H., Tark, K.C., Rah, D.K. and Hong, J.P. **Effect of Recombinant Human Epidermal Growth Factor Against Cutaneous Scar Formation in Murine Full-thickness Wound Healing**. *Journal of Korean Medical Sciences*, 2010; **25**: 589-596.

King, T., Schwarz, M., Brown, K., Tooze, J., Colby, T., Waldron, J., Flint, A., Thurlbeck, W. and Cherniack, R.**Idiopathic Pulmonary Fibrosis: Relationship between Histopathologic Features and Mortality**. *Respiratory and Critical Care Medicine*, 2001; **164**: 1025-1032.

Kohan, M., Muro, A., White, E. and Berkman, N. **EDA-containing cellular fibronectin induces fibroblast differentiation through binding to α4β7 integrin receptor and MAPK/Erk ½-dependent signaling.** J*ournal of the Federation of American Societies for Experimental Biology*, 2010.

Kortylewski, M., Feld, F., Kruger, K., Bahrenberg, G., Roth, R., Joost, H., Heinrich, P., Behrmann, I. and Barthel, A. **Akt Modulates STAT3-mediated Gene Expression through a FKHR (FOXO1a)-dependent Mechanism.** *The Journal of Biological Chemistry*, 2002; **278**: 5242-5249.

Korzus, E., Nagase, H., Rydell, R. and Travis, J. **The Mitogen-activated Protein Kinase and**

JAK-STAT3 Signaling Pathways Are Required for an Oncostatin M-Responsive Element-mediated Activation of Matrix Metalloproteinase 1 Gene Expression. *The Journal of Biological Chemistry*, 1997; **272**(2): 1188-1196.

Karmouty-Quintana, H., Cannet, C., Zurbruegg, S., Ble, F., Fozard, J., Page, C. and Beckmann, N. **Bleomycin-Induced Lung Injury Asessed Noninvasively and in Spontaneously Breathing Rats by Proton MRI.** *Journal of Magnetic Resonance Imaging*, 2007; **26**: 941-949.

Kovalovich, K., DeAngelis, R.A., Li, W., Furth, E.E., Ciliberto, G. and Taub, R. **Increased toxin-induced liver injury and fibrosis in interleukin-6 deficient mice.** *Hepatology*, 2000; **31**(1): 149-59.

Kuropatwinski, K.K., De Imus, C., Gearing, D., Baumann, H. and Mosley, B. **Influence of subunit combinations on signaling by receptors for oncostatin M, leukemia inhibitory factor, and interleukin-6.** *Journal of Biological Chemistry,* 1997; **272**(24): 15135-15144.

Lim, C.P., Phan, T., Lim, I.J. and Cao, X. **Stat3 contributes to keloid pathogenesis via promoting collagen production, cell proliferation and migration.** *Oncogene*, 2006; **25**:5416-5425.

Lu, T.C., Wang, Z.H., Feng, X., Chuang, P.Y., Fang, W., Shen, Y., Levy, D.E., Xiong,H., Chen, N. and He, J.C. **Knockdown of Stat3 activity in vivo prevents diabetic glomerulopathy.** *Kidney International*, 2009; **76**: 63-71.

Mao, Y. and Schwarzbauer, J.E. **Fibronectin fibrillogenesis, a cell-mediated matrix assembly process.** *Matrix biology: Journal of the International Society for Matrix Biology*, 2005; **24**(6): 389-399.

Matsui, T., Kinoshita, T., Hirano, T., Yokota, T. and Miyajima, A. **STAT3 down-regulates the expression of cyclin D during liver development.** *Journal of Biological Chemistry*, 2002; **277**(39): 36167-36173.

Maritano, D., Sugrue, M., Tininini, S., Dewilde, S., Strobl, B., Fu, X., Murray-Tait, V. , Chiarle, R. and Poli, V. **The STAT3 isoforms α and β have unique and specific functions**. *Nature Immunology*, 2004; **5**: 401-409.

McCallion, R.L. and Ferguson, M.W.J. **Scar-Free Embryonic Wound Healing and the Prevention of Scarring Following Wound Healing in the Adult.** *Journal of Theoretical Medicine* 1997; 1: 1-11.

McWhinnie, R., Pechkovsky, D.V., Zhou, D., Lane, D., Halayko, A.J., Knight, D.A. and Bai, T.R. **Endothelin-1 induces hypertrophy and inhibits apoptosis in human airway smooth muscle cells.** *American Journal of Physiology. Lung Cellular and Molecular Physiology,* 2007;

292(1): L278-L286.

Merchant, J.L. **What lurks beneath: IL-11, via Stat3, promotes inflammation-associated gastric tumorigenesis.** *The Journal of Clinical Investigation*, 2008; **118**(5): 1628-1631.

Miles, S.A., Martinez-Maza, O., Rezai, A., Magpantay, L., Kishimoto, T., Nakamura, S., Radka, S.F. and Linsley, P.S. **Oncostatin M as a potent mitogen for AIDS-Kaposi's sarcoma-derived cells**. *Science,* 1992; **255**:1432–1434.

Moodley, Y.P., Misso, N.L., Scaffidi, A.K., Fogel-Petrovic, M, McAnulty, R.J., Laurent, G.J., Thompson, P.J. and Knight, D.A. **Inverse effects of interleukin-6 on apoptosis of fibroblasts from pulmonary fibrosis and normal lungs.** *American Journal of Respiratory Cell and Molecular Biology*, 2003; **29**(4): 490-498.

Moodley, Y.P., Scaffidi, A.K., Misso, N.L., Keerthisingam, C., McAnuity, R.J., Laurent, G.J., Mutsaers, S.E., Thompson, P.J. and Knight, D.A. **Fibroblasts isolated from Normal Lungs and Those from Idiopathic Pulmonary Fibrosis Differ in Interleukin-6/gp130-Mediated Cell Signaling and Proβeration.** *American Journal of Pathology*, 2003; **163**(1): 345-354.

Nielsen, M., Kaestel, C.G., Eriksen, K.W., Woetmann, A., Stokkedal, T., Kaltoft, K., Geisler, C., Ropke, C. and Odum, N. **Inhibition of constitutively activated Stat3 correlates with altered Bcl-2/Bax expression and induction of apoptosis in mycosis fungoides tumor cells.** *Leukemia*, 1999; **13**(5): 735-738.

Nishimoto, N., Ogata, A., Shima, Y., Tani, Y., Ogawa, H., Nakagawa, M., Sugiyama, H., Yoshizaki, K. and Kishimoto, T. **Oncostatin M, leukemia inhibitory factor, and interleukin 6 induce the proliferation of human plasmacytoma cells via the common signal transducer, gp130.** *Journal of Experimental Medicine*, 1994; **179**:1343–134.

Odenthal, M., Neubauer, K., Meyer, K. and Ramadori, G. Localization and mRNA steady-state level of cellular fibronetin in rat liver undergoing a CCl4-induced acute damage or fibrosis. Molecular Basis of Disease, 1993; 1181(3): 266-272.Ogata, H., Chinen, T., Yoshida, T., Kinjyo, I., Takaesu, G., Shiraishi, H., Lida, M., Kobayashi, T and Yoshimura, **A. Loss of SOCS3 in the liver promotes fibrosis by enhancing STAT3-mediated TGFβ1 production.** *Oncogene*, 2006; **25**(17): 2520-2530.

Ono, A., Utsugi, M., Masubuchi, K., Ishizuka, T., Kawata, T., Shimizu, Y., Hisada, T., Hamuro, J., Mori, M. and Dobashi, K. **Glutathione redox regulates TGF-β-induced fibrogenic effects through Smad3 activation.** *Federation of European Biochemical Societies*, 2008; **583**: 357-362.

Pang, M., Kothapally, J., Mao, H., Tolbert, E., Ponnusamy, M., Chin, Y.E. and Zhuang, S. Inhibition of histone deacetylase activity attenuates renal fibroblast activation and interstitial

fibrosis in obstructive nephropathy. American Journal of Physiology, Renal Physiology, 2009; 297(4): F996-F1005.

Pang, M., Ma, L., Gong, R., Tolbert, E., Mao, H., Ponnusamy, M., Chin, E., Yan, H., Dworkin, L. and Zhuang, S. **A novel STAT3 inhibitor, S3I-201, attenuates renal interstitial fibroblast activation and interstitial fibrosis in obstructive nephropathy.** *Kidney Internation*al, 2010; **78**: 257-268.

Pankov, R. and Yamada, K. **Fibronectin at a glance.** *Journal of Cell Science*, 2002; **115**: 3861-3863.

Pechkovsky, D., Hackett, T., An, S., Shaheen, F., Murray, L. and Knight, D. **Human Lung Parenchyma but not Proximal Bronchi Produces Fibroblasts with Enhanced TGFbeta Signaling and alphaSMA Expression.** *American Journal of Respiratory Cell and Molecular Biology*, 2010; Epub.

Singh, P., Carraher, C. and Schwarzbauer, J. **Assembly of Fibronectin Extracellular Matrix.** *Annual Review of Cell and Developmental Biology*, 2010; **26**: 397-419.

Rosenbloom, J., Castro, S. and Jimenez, S. **Narrative Review: Fibrotic Diseases: Cellular and Molecular Mechanisms and Novel Therapies.** *Annals of Internal Medicine*, 2010; **153**(3): 159-167.

Scaffidi, A.K., Mutsaers, S.E., Moodley, Y.P., McAnulty, R.J., Laurent, G.J., Thompson, P.J., Knight, D.A. **Oncostatin M stimulates proliferation, induces collagen production and inhibits apoptosis of human lung fibroblasts.** *British Journal of Pharmacology*, 2002; **136**(5): 793-801.

Schaefer, T., Sanders, L., Park, O. and Nathans, D. **Functional Differences between Stat3α and Stat3β.** *Molecular and Cellular Biology*, 1997; **17**(9): 5307-5316.

Schwartzkopff, B., Fassbach, M., Pelzer, B., Brehm, M. and Strauer, B. **Elevated serum markers of collagen degradation in patients with mild to moderate dilated cardiomyopathy.** *European Journal of Heart Failure*, 2002; **4**(4): 439-444.

Shain, K., Yarde, D., Meads, M., Huang, M., Jove, R., Hazlehurst, L. and Dalton, W. **β1 Integrin Adhesion Enhances IL-6-Mediated STAT3 Signaling in Myeloma Cells: Implications for Microenvironment Influence on Tumor Survival and Proliferation.** *Cancer Research*, 2009; **69** (3): 1009-1015.

Snyder, M., Huang, X.Y. and Zhang, J.J. **Identification of Novel Direct Stat3 Target Genes for Control of Growth and Differentiation.** *The Journal of Biological Chemistry*, 2007; **283**(7): 3791-3798.

Song, H., Wang, R., Wang, S. and Lin, J. **A low-molecular-weight compound discovered through virtual database screening inhibits Stat3 function in breast cancer cells.** *Proceedings of the National Academy of Sciences*, 2005; **102**(3): 4700-4705.

Streetz, K.L., Wustefeld, T, Klein, C., Kallen, K.J., Tronche, F., Betz, U.A., Schutz, G., Manns, M.P., Muller, W. and Trautwein, C. **Lack of gp130 expression in hepatocytes promotes liver injury.** *Gastroenterology*, 2003; **125**(2): 532-543.

Taga, T. and Kishimoto, T. **Gp130 and the interleukin-6 family of cytokines**. *Annual Review of Immunlogy*, 1997; **15**: 797-819.

Takeda, K., Noguchi, K., Shi, W., Tanaka, T., Matsumoto, M., Yoshida, N., Kishimoto, T. and Akira, S. **Targeted disruption of the mouse Stat3 gene leads to early embryonic lethality.** *Proceedings of the National Academy of Sciences*, 1997; **94**(8): 3801-3804.

Tanaka, M. and Miyajima, A. **Oncostatin M, a multifunctional cytokine**. *Reviews of Physiology, Biochemistry and Pharmacology*, 2003; **149**: 39-52.

Tarvady, S., Anguli, V.C. and Pichappa, C.V. **Effect of heparin on wound healing.** *Journal of Biosciences*, 1987; **12**(1): 33-40.

Thomas, A., Lane, K., Philips, J., Prince, M., Markin, C., Speer, M., Schwartz, D., Gaddipati, R., Marney, A., Johnson, J., Roberts, R., Haines, J., Stahlman, M. and Loyd, J. **Heterozygosity for a Surfactant Protein C Gene Mutation Associated with Usual Interstitial Pneumonitis and Cellular Nonspecific Interstitial Pneumonitis in One Kindred.** *Respiratory and Critical Care Medicine,* 2002; **165**: 1322-1328.

Tomasek, J.J., Gabbiani, G., Hinz, B., Chapponnier, C. and Brown, R.A. **Myofibroblasts and mechano-regulation of connective tissue remodelling.** *Nature reviews: Molecular Cell Biology, 2002*; **3**(5): 349-363.

Turkson, J., Bowman, T., Adnane, J., Zhang, Y., Djeu, J., Sekharam, M., Frank, D., Holzman, L., Wu, J., Sebti, S. and Jove, R. **Requirement for Ras/Rac1-Mediated p38 and c-Jun N-Terminal Kinase Signaling in Stat3 Transcriptional Activity Induced by the Src Oncoprotein.** *Molecular and Cellular Biology*, 1999; **19**(11): 7519-7528.

Turkson, J. and Jove, R. **STAT proteins: novel molecular targets for cancer drug discovery.** *Oncogene*, 2000; **19**(56): 6613-6626.

Valenick, L., Hsia, H. and Schwarzbauer, J. **Fibronectin fragmentation promotes α4β1 integrin-mediated contraction of a fibron-fibronectin provisional matrix.** *Experimental Cell Research*, 2005; **309**(1): 48-55.

Vlodavsky, I., Korner, G., Ishai-Michaeli, R., Bashkin, P., Bar-Shavit, R. and Fuks, Z. **Extracellular matrix-resident growth factors and enzymes: possible involvement in tumor metastasis and angiogenesis.** *Cancer Metastasis Review*, 1990; **9**(3): 203-226.

Westergren-Thorsson, G., Hernnas, J., Sarnstrand, B., Oldberg, A., Heinegard, D. and Malmstrom, A. **Altered expression of small proteoglycans, collagen, and transforming growth factor-beta 1 in developing bleomycin-induced pulmonary fibrosis in rats.** *The Journal of Clinical Investigation*, 1993; **92**(2): 632-637.

Williams, C.M., Engler, A.J., Slone, R.D., Galante, L.L. and Schwarzbauer, J.E. **Fibronectin expression modulates mammary epithelial cell proliferation during acinar differentiation.** *Cancer Research*, 2008; **68**(9): 3185-3192.

Yan, Z., Liu, Z. and Chen, Y. **Regulation of TGF-β signalling by Smad7.** *Acta Biochmica et Biophyica Sinica*, 2009; **41**(4): 263-272.

Zhang, X., Wrzeszczynska, M., Horvath, C. and Darnell, J. **Interacting Regions in Stat3 and c-Jun That Participate in Cooperative Transcriptional Activation.** *Molecular and Cellular Biology*, 1999; **19**(10): 7138-7146.

APPENDIX – Cell confluency and STAT3 activity

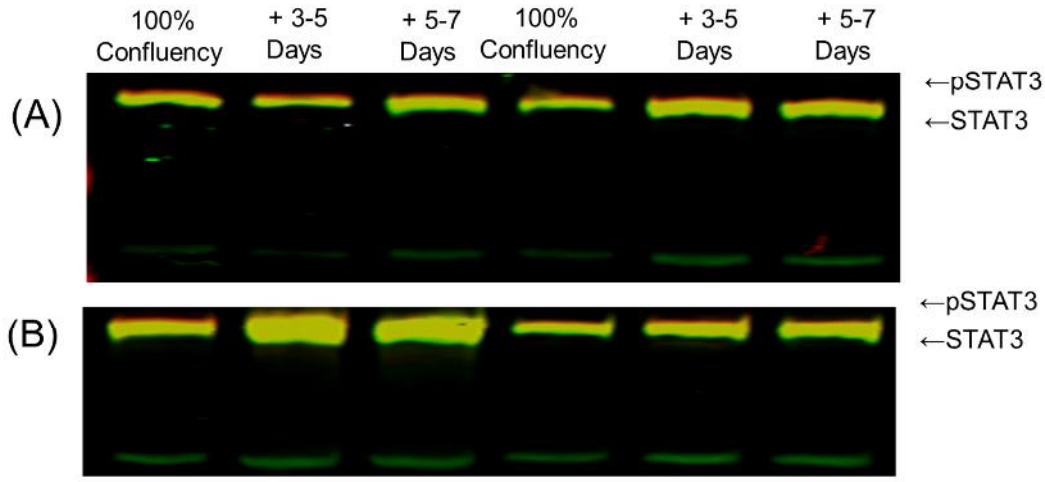

Western Blot of pSTAT3 and STAT3 (90 kDa) levels at varying cell confluency in untreated (A) lung fibroblasts and (B) bronchial fibroblasts. B-tubulin (50 kDa) was included as a control constitutive housekeeping protein.

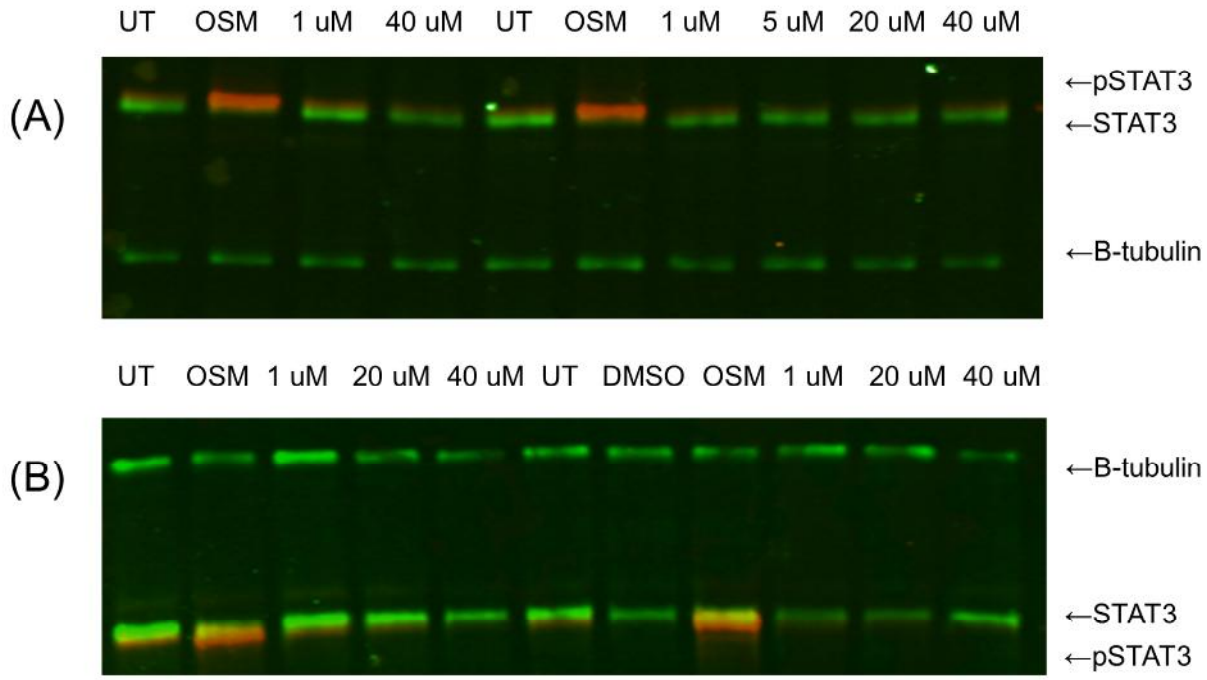

Western blot of pSTAT3 and STAT3 levels at each STA-21 concentration in lung fibroblasts compared to untreated (UT), oncostatin-M (OSM) and DMSO controls at (A) 24 hours and (B) 72 hours. B-tubulin was included as a control constitutive housekeeping protein.